Designed sponges based on chitosan and cyclodextrin polymer for a local release of ciprofloxacin in diabetic foot infections

A. Gauzit Amiel, C. Palomino-Durand, M. Maton, M. Lopez, F. Cazaux, F. Chai, C. Neut, B. Foligné, B. Martel, N. Blanchemain

Designed sponges based on chitosan and cyclodextrin polymer for a local release of ciprofloxacin in diabetic foot infections

A. Gauzit Amiel[a], C. Palomino-Durand[a], M. Maton[a], M. Lopez[a], F. Cazaux[b], F. Chai[a], C. Neut[c], B. Foligné[c], B. Martel[b], N. Blanchemain[a]

a. Univ. Lille, INSERM, CHU Lille, U1008 - Controlled Drug Delivery Systems and Biomaterials, F-59000 Lille, France

b. Univ. Lille, CNRS, INRAE, Centrale Lille, UMR 8207 - UMET - Unité Matériaux et Transformations, F-59000 Lille, France

c. Univ. Lille, INSERM, CHU Lille, U1286 - INFINITE- Institute for Translational Research in Inflammation*, F-59000 Lille, France*

Corresponding author

Dr. Nicolas Blanchemain

E-mail: nicolas.blanchemain@univ-lille.fr

Address: INSERM U1008, Controlled Drug Delivery Systems and Biomaterials, College of Pharmacy, University of Lille, 59006 Lille, France

Tel.: +33 320 62 69 75

Fax: +33 320 62 68 54

Declarations of interest: None

Abstract

Diabetic foot infections are the most common complications requiring hospitalisation of patients with diabetes. They often result in amputation to extremities and are associated with high morbi-mortality rates, especially when bone is infected. Treatment of these complications is based on surgical procedures, nursing care and systemic antibiotic therapy for several weeks, with a significant risk of relapse. Due to low blood flow and damage caused by diabetic foot infection, blood supply is decreased, causing low antibiotic diffusion in the infected site and an increase of possible bacterial resistance, making this type of infection particularly difficult to treat. In this context, the aim of this work was to develop a medical device for local antibiotic release. The device is a lyophilized physical hydrogel, *i.e* a sponge based on two oppositely charged polyelectrolytes (chitosan and poly(cyclodextrin citrate)). Cyclodextrins, via inclusion complexes, increase drug bioavailability and allow an extended release. Using local release administration increases concentrations in the wound without risk of toxicity to the body and prevents the emergence of resistant bacteria. The hydrogel was characterised by rheology. After freeze-drying, a curing process was implemented. The swelling rate and cell viability were evaluated, and finally, the sponge was impregnated with a ciprofloxacin solution to evaluate its drug release profile and its antibacterial activity.

Keywords: diabetic foot infection, chitosan, cyclodextrin polymer, polyelectrolyte complex, ciprofloxacin, sponge

1. Introduction

Deep bone infections are particularly serious, requiring multidisciplinary care, and yet still remains difficult to cure. There are several types of deep bone infections; like osteo-articular infections, infections on osteosynthesis materials, spondylodiscitis, osteitis and diabetic foot infections (DFI), with the latter being extremely difficult to treat. With these issues only expected to increase in the future (629 million diabetics persons in 2045 according to the international diabetes federation), DFI are a public health problem due to their frequency and to the high cost generated by their treatment (Uçkay et al., 2015)(Lipsky et al., 2016)(Volmer-Thole and Lobmann, 2016). Diabetic neuropathies are the gateway for these infections. They cause a decrease of peripheral sensations and lead to foot wounds and deformities (Noel et al., 2010). Moreover, arteriopathy diseases and immune deficiency raise the risk of infection. Low blood flow in the bone, *i.e.* ischemia, surrounding sclerotic tissue, and the presence of biofilms, decrease antibiotic penetration and compromise treatment of these infections, subsequently leading to amputation, morbidity and high mortality (Noel et al., 2010)(Winkler and Haiden, 2016). To eradicate these infections, antibiotics need to be delivered by systemic routes, at higher doses than normally recommended, which may lead to toxic side effects. To solve this clinical concern, the scientific community is now looking for new vectors for topical distribution of drugs to the wound in addition to existing systemic administrations, in order to overcome problems of avascularisation, low diffusion in the bone and antimicrobial resistance selection (Noel et al., 2010)(Winkler and Haiden, 2016). In the therapy of diabetic foot infection, there is currently no standard treatment pathway, however we can see three main treatment options generally adopted by medical practitioners for foot infection treatment. This includes polymethylmethacrylate (PMMA) spacers, calcium sulfate beads and collagen sponges impregnated with antibiotics (Roeder et al., 2000)(Roeder et al., 2000)(Karr, 2011)(Morley et al., 2016)(Gauland, 2011)(Uçkay et al., 2018a)(Uçkay et al., 2018b)(Costa Almeida, 2016).

Among drug carrier scaffolds, hydrogels and sponges are good candidates to act as drug delivery vectors due to their biocompatibility, biodegradability, swelling properties to fill a defect, and drug sorption properties (Li et al., 2019)(Li and Mooney, 2016)(Matsumine et al., 2019). Hydrogels can be obtained through chemical or physical crosslinking routes. Chemical crosslinking of chitosan based hydrogels is often based on a reaction often using glutaraldehyde or genipin, and present the drawback to release unreacted toxic components (Moura et al., 2011). On the other hand, physical hydrogels are formed by polymer networks crosslinked by non-covalent and reversible bonds such as hydrogen and hydrophobic bonds, through ionic interactions between polyelectrolytes with divalent

metals such as Ca^{2+} or with polycarboxylic acids such as citric acid, or by a combination of oppositely charged interpenetrated polyelectrolytes networks. Among these, chitosan (CHT) is widely used in pharmaceutical fields due to its biocompatibility, biodegradability, antibacterial and antifungal properties and drug delivery properties (Noel et al., 2010)(Kong et al., 2010)(Stinner et al., 2010)(Mittal et al., 2018). CHT is obtained from chitin deacetylation. Chitin is extracted from arthropod exoskeletons, crustaceans and some molluscs. Natural CHT can also be found in some fungi cell walls. These sources are inexpensive, making chitin and therefore chitosan very attractive materials for the biomaterials industry (Moura et al., 2013). CHT is a natural polysaccharide consisting of glucosamine and N-acetyl glucosamine units linked by *β*-(1→4) glycosidic bonds (figure 1). CHT is the only biologically sourced cationic polysaccharide that can form physical hydrogels with a large amount of anionic polysaccharide through the formation of polyelectrolyte complexes (PEC) (Luo and Wang, 2014).

Cyclodextrins (CDs) are natural macrocyclic oligosaccharide molecules linked by α-1→4 glycosidic bonds, derived from starch. More precisely, they are called α, *β* and ɣ-CD depending on the number of glucopyranose units they are composed of, respectively 6, 7 or 8. Their toroidal structure with a hydrophilic outer surface and a lipophilic cavity gives them the ability to form an inclusion complex with a variety of compounds (Loftsson et al., 2005). Thereby, they are widely used for pharmaceutical purposes in order to increase drug solubility and stability, to prolong drug release and to improve drug permeability through biological barriers (Loftsson et al., 2005)(Machín et al., 2012)(Monnaert et al., 2004). Furthermore, the low toxicity and low immunogenicity of cyclodextrins make them very attractive for biomedical applications (Zhang and Ma, 2013). Cyclodextrin polymers (PCD) were developed more recently due to their mechanical properties, stimuli-responsiveness and drug release characteristics (van de Manakker et al., 2009). Among these polymers, our group synthetized a crosslinked water-soluble poly(cyclodextrin citrate) (figure 1) (Martel et al., 2005). Due to the residual carboxylic functions carried by the citrate crosslinks (in the range of 4 mmol/g), these types of PCD are considered as anionic polymers, allowing PEC formations with CHT (figure 1). Our laboratory has recently developed drug release systems based on PEC formed between CHT and PCD. In our first system we applied layer-by-layer assemblies on textile or on metal surfaces (Martin et al., 2013a)(Martin et al., 2013b)(Pérez-Anes et al., 2015)(Aubert-Viard et al., 2019). We then used a PEC formation to prepare nanofiber membranes for drug delivery by electrospinning (Ouerghemmi et al., 2016). Finally, we developed a CHT and PCD physical hydrogel for a tissue engineering application, and a sponge with antibacterial properties as a wound dressing (Palomino-Durand et al., 2019)(Flores et al., 2017). We successfully obtained sponges with the combination of CHT and PCD but without good stability and mechanical properties for an application in DFI. The challenge here is to stabilise the microporous sponge structure without losing the beneficial drug delivery properties in presence

of physiological fluids. So in the present paper we expose the manufacturing process of this physical CHT:PCD sponge. After characterisation by rheology of 3:0, 3:1, 3:3, 3:5 and 3:7 ratios, hydrogels are freeze-dried into sponges. The aim of this work was to evaluate the impact of a thermal treatment (TT) on the properties of the sponges for our clinical application. The mechanical properties and the structure of the sponges were analysed. In order to study the ability to use these sponges for deep irregular wounds like DFI, they were loaded with ciprofloxacin (CIP) and we studied their drug release profiles and antibacterial activities *in vitro* by a diffusion test.

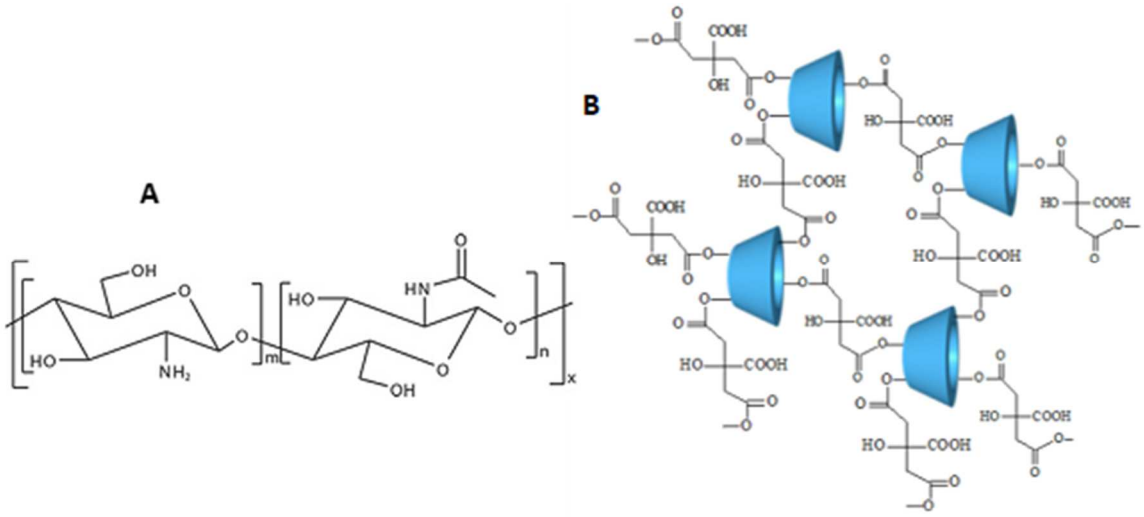

Figure 1 : Structure of cationic CHT (A) and poly(cyclodextrin citrate) PCD (B)

2. Materials and methods

2.1. Materials

CHT (batch STBG1894V, Mw: 190 kDA, DD: 73 %) was provided from Sigma Aldrich (France). Poly(cyclodextrin citrate) (PCD, Mw: 26.8 kDa, cyclodextrins percentage: 58 %) was synthesised in our laboratory as described by Martel et al (Martel et al., 2005). Water soluble PCD is obtained by the polymerisation between *β*CD (Kleptose ®, Roquette, Lestrem, France) and citric acid (Sigma Aldrich, France) in the presence of sodium hypophosphite (Sigma Aldrich, France) as a catalyst. The molar mass was 20 kDa, determined by size exclusion chromatography with refractive index and dynamic light scattering detectors. The cyclodextrin weight percentage was determined by 1H NMR, composed of 58%. Phosphate buffered saline (PBS, pH 7.4, Sigma Aldrich, France) was prepared by solubilisation of one tablet (200 mg) in 1 litre of ultra-pure water. Ultra-pure water (18.2 MΩ.cm) was purified by EGLA VEOLIA system (Purelab flex, ELGA, UK). Glacial acetic acid (Merck, France) was

used to solubilise CHT where the antibiotic ciprofloxacin (200 mg/100mL, Fresenius Kabi, France) was used to load the sponges.

2.2. Methods

2.2.1. Hydrogels and Sponges preparation

Sponges were obtained from freeze-dried hydrogels according to a process previously described by our teams (Flores et al., 2017)(Blanchemain et al., 2017). In a preliminary step, raw CHT powder was grinded with a variable-speed rotor mill (Pulverisette 14, Fritsch, Germany) through a 125 µm sieve ring, and PCD powder was milled in a mortar. After sieving at 125 µm, the powders of CHT:PCD ratios were co-milled in a mixer mill MM-400 (Retsch, Germany) at 10 Hz for 3 min. Hydrogel formulations are presented in Table 1.

The preparation of physical CHT:PCD hydrogels (figure 2) were carried out using a system of two connected syringes. Co-milled powders were loaded in the first syringe and ultra-pure water in the other. Both syringes were connected by a luer-lock female-female connector (Vygon®, France), mixed the powders and water thoroughly by pressing alternately on each of the plungers for 1 min and 30 sec, after which pure acetic acid was added to the mixture (for a final concentration of 1 %) using the above-mentioned process. The physical hydrogel obtained was injected into a mould (Falcon centrifuge PP tube ∅ 11 mm x 7,5 cm, BD Biosciences, France), frozen for 12 hours at -20 °C and finally lyophilised for 48 hours at 0,06 mBar and -55 °C (Christ alpha 1-2 LD, Osterode am Harz, Allemagne). For each ratio, half of the CHT:PCD sponges were cured in an oven UFP600 (Memmert, France) at 140 °C for 1h30. Thermal treated (TT) and non-thermal treated (NTT) sponge behaviours were evaluated.

Table 1 : Presentation of CHT:PCD hydrogels formulations expressed in g of powder/100 cm³ in the final mixture. CHT=Chitosan, PCD= Soluble poly(cyclodextrin citrate), AcOH=acetic acid

CHT:PCD	CHT %, w/v	PCD %, w/v	Water %, v/v	AcOH %, v/v
3:0 (control)	3	0	96	1
3:1	3	1	95	1
3:3	3	3	93	1
3:5	3	5	91	1
3:7	3	7	89	1

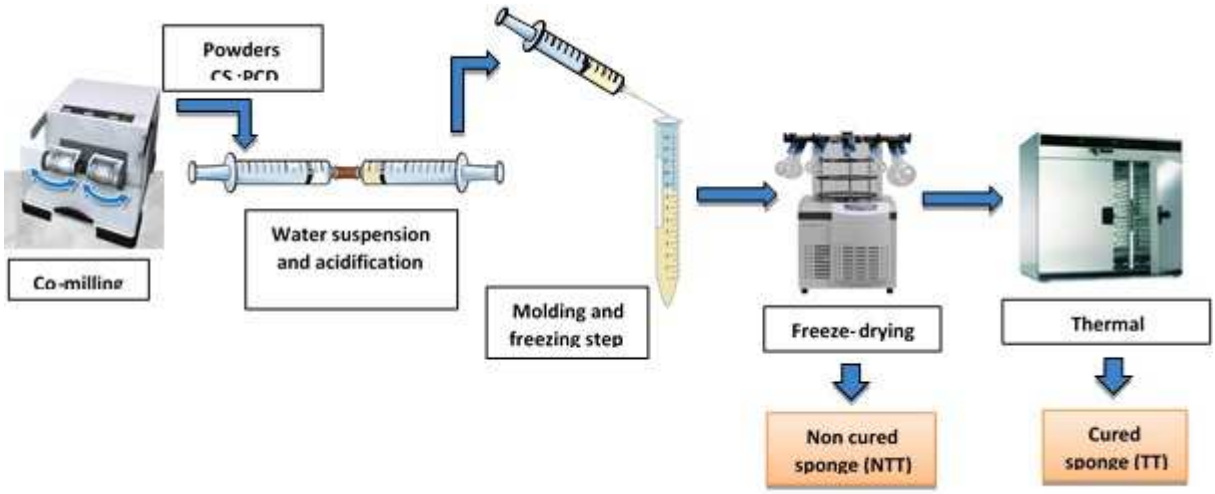

Figure 2 : Protocol of fabrication of hydrogels and sponges (TT and NTT)

2.2.2. Hydrogel characterisations

A reverse vial test was done for a qualitative evaluation of gelation (Raghavan and Cipriano, 2006). After preparation in the interconnected syringes, a hydrogel mixture was immediately injected into a vial and turned upside-down to evaluate samples stability or flowing behaviour after incubation at 37 °C for 0 h, 1 h and 24 h. for each CHT:PCD ratio.

Rheological analyses were performed on the hydrogel mixtures to assess their viscoelastic properties. Measurements were performed by using an MCR 301 rheometer (Anton Paar, France) with a parallel plate geometry of 25 mm diameter (PP25, Anton Paar), a Peltier plate for temperature control, and a plate cover to prevent water evaporation during analyses. A gap of 1 mm was fixed for all measurements, and fresh hydrogels were loaded into the syringes immediately after the mixing process. The linear viscoelastic range (LVR) was determined in a strain sweep program at a constant frequency (1 Hz). Hydrogel storage (G') and loss (G'') moduli were evaluated as a function of time at 37 C° in the oscillatory mode at 1 Hz frequency and 1% strain. Angular frequency sweep analyses were carried out at 1 % strain from 1-100 rad.s^{-1} at RT. All tests were performed in triplicate.

2.2.3. Sponge characterisations

Scanning Electron Microscopy (SEM, S-4700 field emission GU, Hitachi, Germany) was used to evaluate the morphology of the sponges. Accelerating voltage was set up at 5 kV and the emission current at 10 µA (magnification x50). Samples were chrome coated before observations. Due to the

heterogeneous shape of the pores of the sponge, a size analysis was performed by measuring the diameter of 20 pores randomly selected using the software ImageJ.

Swelling properties were assessed with dry cylindrical sponges (∅11 mm x 5 mm). Sponges were weighed and immersed in a PBS solution (10 mL per 20 mg of sponges) at 37 °C and 80 rpm. At regular time intervals (30 min and every hour for 6 hours with a final weighing at 24 h), the sponges were collected, dried on an absorbent paper tissue and weighed. Swelling rate was determined by the formula $\frac{mt-m0}{m0} * 100$ (*mt*: sample humid mass at specific time, *m0*: sample dry mass before swelling) (Flores et al., 2017). Swelling measurements were made at room temperature and in triplicate.

Mechanical tests were performed with a CellScale Univert® (Waterloo, Canada). Cylindrical samples (∅11 mm x 11 mm) were swelled for 4 hours in PBS (37 °C, 80 rpm) and were squeezed up to 50% of their initial size. Compression force was measured using a 10 N cell. Compressive modulus were calculated as the gradient of the initial linear portion in the stress-strain curve and initial shape recovery was then recorded during the release of the compression force. Measurements were assessed in triplicate for each formulation.

Degradation behaviour was evaluated on cylindrical sponges (∅ 6 mm x 5 mm) after 7 days in PBS. Dried sponges were weighed and hydrated in 5 mL of PBS at 37 °C and 80 rpm. Samples were dipped in a degradation medium and collected after 2 h, 6 h, 24 h, 48 h, 5 and 7 days, after each time frame they were freeze-dried and weighed. Degradation rate was established by the formula $100 - (\frac{m_0-m_t}{m_0} * 100)$ (m_0: sample weight at t_0, m_t: sample weight after *t* hours of degradation) (Endogan Tanir et al., 2015).

Enzymatic degradations of the sponges were performed in a PBS solution supplemented with 0,5 mg/mL of sodium azide (Sigma Aldrich, Germany) and 0,5 mg/mL of lysozyme (Fluka, Sigma Aldrich, Belgium). Degradation mediums were changed every 2 days (Endogan Tanir et al., 2015). Degradation rates were established by the formula $100 - (\frac{m_0-m_t}{m_0} * 100)$ (m_t: sample weight after *t* hours of degradation, m_0: sample weight at t_0) (Endogan Tanir et al., 2015). Tests were realised in triplicate.

2.2.4. Ciprofloxacin (CIP) kinetic release study

Cylindric sponges (∅11 mm x 5 mm) were impregnated with 10 mL of a CIP solution protected from light for 4 hours, at 37 °C and 80 rpm. Impregnated sponges were then rinsed in ultra-pure water (10 mL, 10 sec, 240 rpm) to remove non-fixed CIP.

Kinetic release studies were performed in static conditions. Release tests was performed in a sterile environment. Sponges were immersed in 5 mL of sterile PBS and stirred at 80 rpm at 37 °C. Every 6 hours and then at 24 h, 72 h and 96 h, 1 mL of medium was collected and refreshed. 950 µL of this medium was filtered and dosed by HPLC (Shimadzu LC2010, France). A reversed phase Gemini column C18 150 x 3 mm was used as a stationary phase, with a 5 µm granulometry and a 110 Å porosity (Phenomenex, USA). The mobile phase was a mixture of acetic acid and acetonitrile in the proportions 87/13, (v/v) with a 1 mL/min flow. UV detection was performed at a 271 nm wavelength. The remaining 50 µL were kept for microbiological tests. Tests were performed on n=6 samples of each formulation.

2.2.5. Biological tests

The antibacterial activity of released medium from CIP loaded sponges was evaluated by an agar diffusion test (Kirby Bauer test) on the reference bacterial strains *Escherichia coli* K12 or *Staphylococcus aureus* ATCC 8147. Bacteria were suspended in 10 mL of a cysteinated Ringer solution in order to obtain a stock suspension with a density of around 10^4 CFU/mL. 0,1 mL of each inoculum were seeded on a Mueller Hinton (ThermoScientific®, Oxoid Microbiological Products, France) agar (Difco®, Fisher Scientific™, France) (18 mL) plate. 50 µL of release medium was injected afterward in wells created equidistantly on the agar plates. The inhibition growth diameter was measured after 24 hours of incubation at 37 °C under aerobic conditions. Experiments were realised 6 times on each sponge formulation.

Sponge cytotoxicity was assessed using MC3T3-E1 pre-osteoblastic cells (CRL-2594™, ATCC®, USA) according to the extraction method ISO 10993-5 Standard. Cell cultures were α-MEM, purchased from Gibco® (Thermo Fisher Scientific, France) supplemented with 10% of FBS (Eurobio, France). The cells were incubated at 37 °C, 5% CO_2 atmosphere and 100% relative humidity in an incubator (CB150/APT Line/Binder, LabExchange, France). Sponges were swelled in α-MEM for 24 hours, at 37 °C and 80 rpm. Then they were removed, weighed, and medium excess was eliminated using a soft absorbent paper tissue, and re-incubated in α-MEM (100 mg/mL) for a further 24 hours in the same conditions for extraction purposes. In parallel, MC3T3-E1 cells were seeded at 4×10^3 cells/well in a 96-well tissue culture polystyrene (TCPS) plate and grown in 100 µL/well MEM-α medium,

supplemented with 10% FBS at 37°C, 5 % CO_2 for 24 hours. This medium was collected and replaced by the extraction medium (filtered through a 0.2 µm sterile syringe filter) and incubated for a final 24 hours (37 °C, 5% CO_2). Lastly, cell viability was determined by AlamarBlue® assay (Uptima, Interchim, France). Briefly, medium was replaced with 200 µL of a 10% solution of AlamarBlue® and the plates were placed, protected from light, for a 2 h incubation at 37 °C, 5% CO_2. 150 µL/well of this solution were transferred to a 90-well plate Fluoro-LumiNunc™ (ThermoScientific, France) and fluorescence was measured by a fluorimetry (Twinkle LB 970 Microplate Fluorometer, Berthold Technologies GmbH & Co, Germany) at a 530 nm excitation wavelength and a 590 nm emission wavelength. Fluorescence readings are proportional to cellular activity, expressed by the percentage of cell viability, and compared to the negative control. N=6 samples were tested three times per ratio.

2.2.6. Statistical analyses

All data was expressed as the means ± standard deviation (SD). Statistical tests were performed by Statplus software (version Build 6.7.1.0/Core v6.2.02). Data was analysed using a one-way ANOVA and a post-hoc Tukey test. The differences were regarded to be statistically significant for $p < 0.05$.

3. Results and discussion

3.1. Hydrogel preparations and characterisations

3.1.1. Macroscopic observations

Hydrogels were prepared from mixed powders of CHT:PCD, where CHT was fixed to 3 %w/v and PCD was varied from 1 to 7 %w/v as described in Table 1. Powder mixtures were weighed and introduced into a syringe. Ultra-pure water was injected from another syringe and blended with the mixture through the Luer-lock connector. Acetic acid was then added to the suspension in water using the same process (figure 2). The formation of a homogeneous viscous solution for all ratios was observed, except for ratio 3:7 which remained liquid with a powder/solvent phase separation.

In order to test the consistency of each formulation, the hydrogel formulations were injected into the bottom of a vial and a reverse vial test was performed. In this test the hydrogels were submitted to gravity force at 37°C and consistency was then evaluated by observing whether the hydrogels flowed or remained at the bottom of the vial at 1h and 24h (Raghavan and Cipriano, 2006). As shown in Figure 3 A, the 3:7 formulation flowed under the effects of gravity immediately after injection and inversion of the vial, where the 3:0 formulation only began to flow after 1 hour (figure 3 B). Hydrogels 3:1, 3:3 and 3:5 did not flow after inversion, even after 24 hours. After this experiment, formulation 3:7 was discarded from the following study and the 3:0 formulation was maintained as a control.

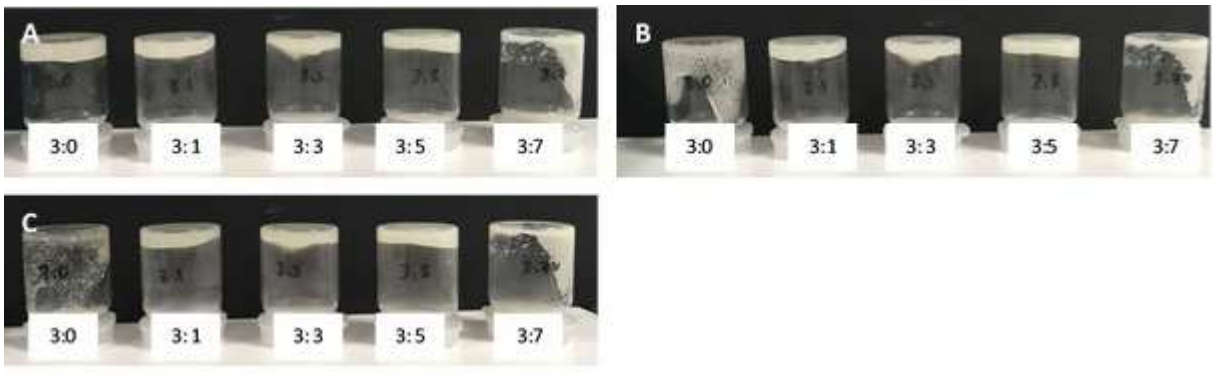

Figure 3 : Inverted-vial test for all ratios, 3:0, 3:1, 3:3, 3:5 and 3:7 just after injection (A), after 1 h (B) and 24 h (C) at 37 °C

3.1.2. Rheological analysis

Hydrogels 3:0, 3:1, 3:3 and 3:5 were prepared and immediately injected onto the rheometer's Peltier device for analysis. The evolution of the hydrogel moduli G' (elastic modulus) and G'' (loss modulus) were measured at 37 °C, according to time and in oscillatory mode with a deformation amplitude of 1 % (figure 4).

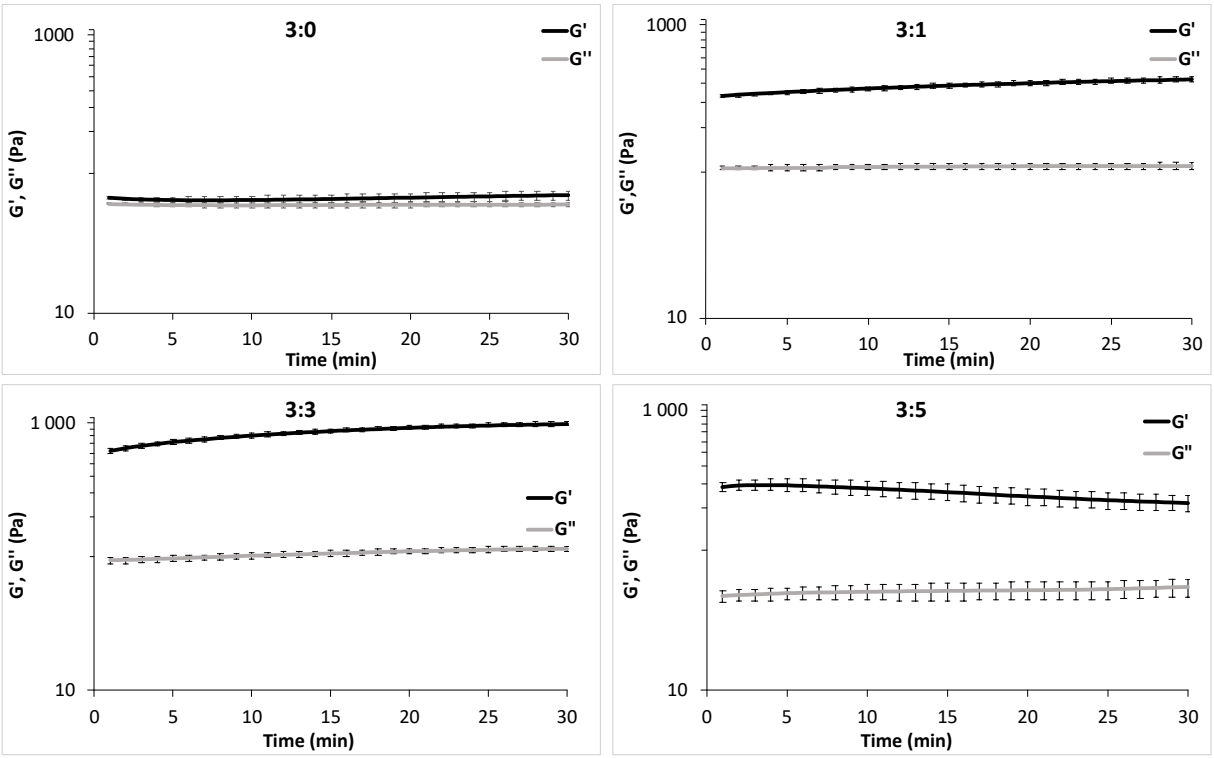

Figure 4 : Time sweep evolution of the storage modulus: G' and loss modulus: G'' of CHT:PCD hydrogels 3:0, 3:1, 3:3 and 3:5 (strain γ=1 %, frequency ω=10 s^{-1}, 37° C). Mean of N=3 samples

Since the beginning of time sweep test, all formulations displayed G' values superior to G'' values. Thus, the hydrogel displayed a viscoelastic behaviour, in which a cohesive gel is instantly formed in the syringe (preformed hydrogel) during the acidification of the suspension with acetic acid (figure 2). We previously reported that the addition of acetic acid causes the protonation of amino groups into ammonium groups leading to the extension of CHT macromolecular chains toward the conformation of extended polymer coils by intramolecular repulsion between positive charges (Flores et al., 2017)(Palomino-Durand et al., 2019). In addition, this solubilisation facilitates ionic interactions between the NH_3^+ groups of CHT and the COO^- groups of soluble PCD to form a PEC (Roy et al., 2017)(Fatimi et al., 2009). Anraku et *al.* also demonstrated the formation of ionic interactions during the preparation of a CHT hydrogel with sulfobutyl ether-CD (Anraku et al., 2015). Their rheological analysis showed the formation of an elastic hydrogel with G' values of approximately 5000 Pa and G'' of 500 Pa (Anraku et al., 2015). In our case, different values of G' and G" were

measured on the different hydrogel formulations. In the four formulations displayed in figure 4, G" values were stable for the 30 minute assay and values were spread in a narrow range of order (40 Pa ≤ G" ≤ 100 Pa). On the contrary, G' displayed a higher variation than G" within the assay, and their ranges of their orders were very different depending on the hydrogel formulations. Hydrogel 3:0 presented G' value within the 65 to 70 Pa respective upper and lower limits, against 320-400 Pa for the 3:1 ratio, 600-1000 Pa for the 3:3 ratio and 250-300 Pa ratio.

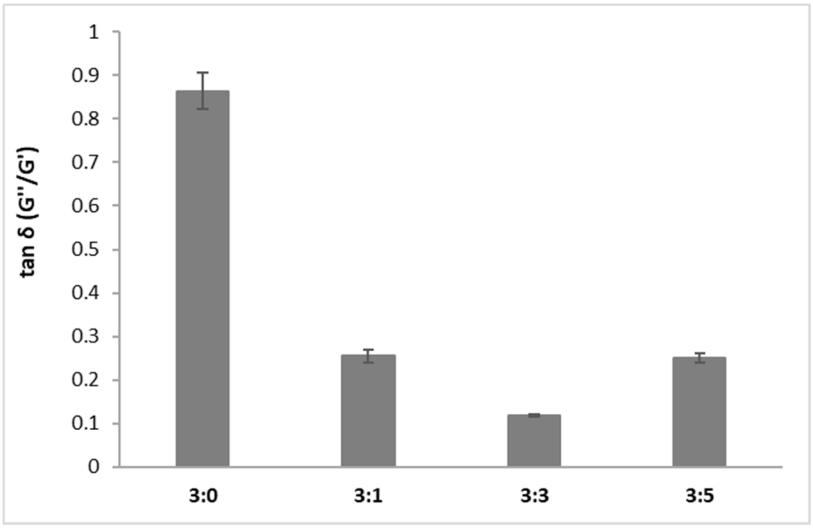

Figure 5 : tan δ values measured at t 30 min for ratios 3:0, 3:1, 3:3 et 3:5 (γ=1 %, ω=10 rad.s^{-1}, 1 mm, 37 °C)

Tan δ calculated from G"/G' is called the *damping factor* and reflects the viscoelastic properties of the polymer-solvent systems. Predominance of viscous liquid or elastic solid character behaviours can be deducted from tan δ values superior or inferior to one, respectively (Borzacchiello and Ambrosio, 2009)(Jin et al., 2009)(Arslan et al., 2018). Furthermore, flowing "weak" hydrogels are characterised by tan δ values superior to 0.1, while non flowing "strong" hydrogels are characterised by tan δ < 0.1 (Borzacchiello and Ambrosio, 2009)(Rogina et al., 2017). In figure 5, the 3:0 formulation of the solution produced intermediate results with tan δ value almost equal to 1. For the 3:3 formulation, a marked decrease of tan δ was observed with the increase of the PCD amount in the formulation, and the minimal value was observed, reaching the value of 0.1. So according to literature, this hydrogel can be classified as having a "strong" hydrogel character, while formulations 3:1 and 3:5 present a "weak" hydrogel character. Hydrogel viscoelastic properties are principally linked with its crosslink density. The content of CHT amino groups and PCD carboxyl groups were determined respectively as 5 mmol/g and 4 mmol/g (Martel et al., 2005)(Martin et al., 2013b). Thus, our results show that the CHT:PCD 3:3 ratio displays the lowest tan δ value meaning that it

corresponds to the optimal balance between positive and negative charges, generating the highest density of electrostatic interactions in the polymeric network.

Table 2 : Amount of ammonium groups and carboxylate groups for hydrogels CHT:PCD, G', G" and tan δ values recorded after 30 minutes

CHT:PCD	NH_3^+ (mmol)	COO^- (mmol)	NH_3^+/COOH ratio	G ' (Pa)	G'' (Pa)	Tan δ
3:0	2.25	0		70 ± 5	61 ± 2	0.86 ± 0,04
3:1	2.25	0.6	3.75	428 ± 19	109 ± 20	0.25 ± 0.02
3:3	2.25	1.8	1.25	990 ± 37	115 ± 34	0.12 ± 0
3:5	2.25	3	0.75	217 ± 27	54 ± 8	0.25 ± 0.01

3.2. Sponges characterisation

3.2.1. Macroscopic observations

After injection into a mould, the hydrogels were frozen and then freeze-dried in order to create microporous materials called sponges. After unmoulding, cylinders (∅ 11 mm, height 5 mm) were cut into slices along the length of the sponge, which was created within the Falcon tube. Macroscopically, their colour was white, and their porosity seemed homogenous. After thermal treatment (TT) at 140 °C, we observed a brown coloration due to the rearranging of CHT chains and the formation of covalent bonds (crosslinking) (Ji and Shi, 2013). Amide bonds are formed at high temperatures between the NH_2 groups of CHT and the COOH groups of PCD. This crosslinking reaction was also demonstrated in our laboratory by Aubert-Viard et *al.* after a heat treatment at 140°C for 105 min of a textile functionalised by a multi-layer system based on a CHT and PCD PEC. They showed that by this treatment, the number of amine functions (determined by orange acid assay) decreased significantly due to the formation of amide bonds between the CHT and carboxylic amine groups of PCD (Aubert-Viard et al., 2019)(Ouerghemmi et al., 2016).

After hydration in PBS solutions, all sponges were easy to handle and showed good mechanical resistance, except for the 3:0 NTT samples which lost its shape. Therefore the 3:0 NTT samples were discarded and only the 3:0 TT sponges were considered.

3.2.2. Scanning electron microscopy

SEM analysis displayed the different sponge microarchitectures. The microarchitecture plays a major role in the absorption capacity of active ingredients. The more porous a substrate is, the greater its absorption capacity is (Wang et al., 2017)(Ramli et al., 2013). In addition, this porosity will promote the circulation of biological fluids through the material.

SEM analyses did not reveal any difference in microstructure between sponges, whether they were heat treated or not (figure 6). A regular and interconnected porous structure was observed for ratios 3:0 TT, 3:1 NTT/TT and 3:3 NTT/TT. However, this alveolar microstructure was affected upon increasing the PCD ratio in the formulation as observed in particular in the 3:5 NTT and TT sponges, compared with 3:0 to 3:5 ratios. So, SEM photos indicate that CHT is responsible for the alveolar morphology of the device. Contrary to chitosan which is a linear polymer, PCD is a globular crosslinked polymer of approximately 50 nm diameter when in a solution (Herbois et al., 2015). In a former paper, we observed that pure PCD lyophilizates form granular powders with no bulk mechanical properties, contrary to chitosan (Garcia-Fernandez et al., 2016). As a consequence, the excess of PCD in the 3:5 sponges disrupted the alveolar structure observed for other formulations. Pore diameter analysis revealed a high heterogeneity for each group (3:0 TT : 176 ± 50 µm, 3:1 TT : 208 ± 67 µm, 3:3 TT : 177 ± 56 µm and 3:5 TT : 165 ± 35 µm) without any significant difference between the formulations ($p > 0.05$).

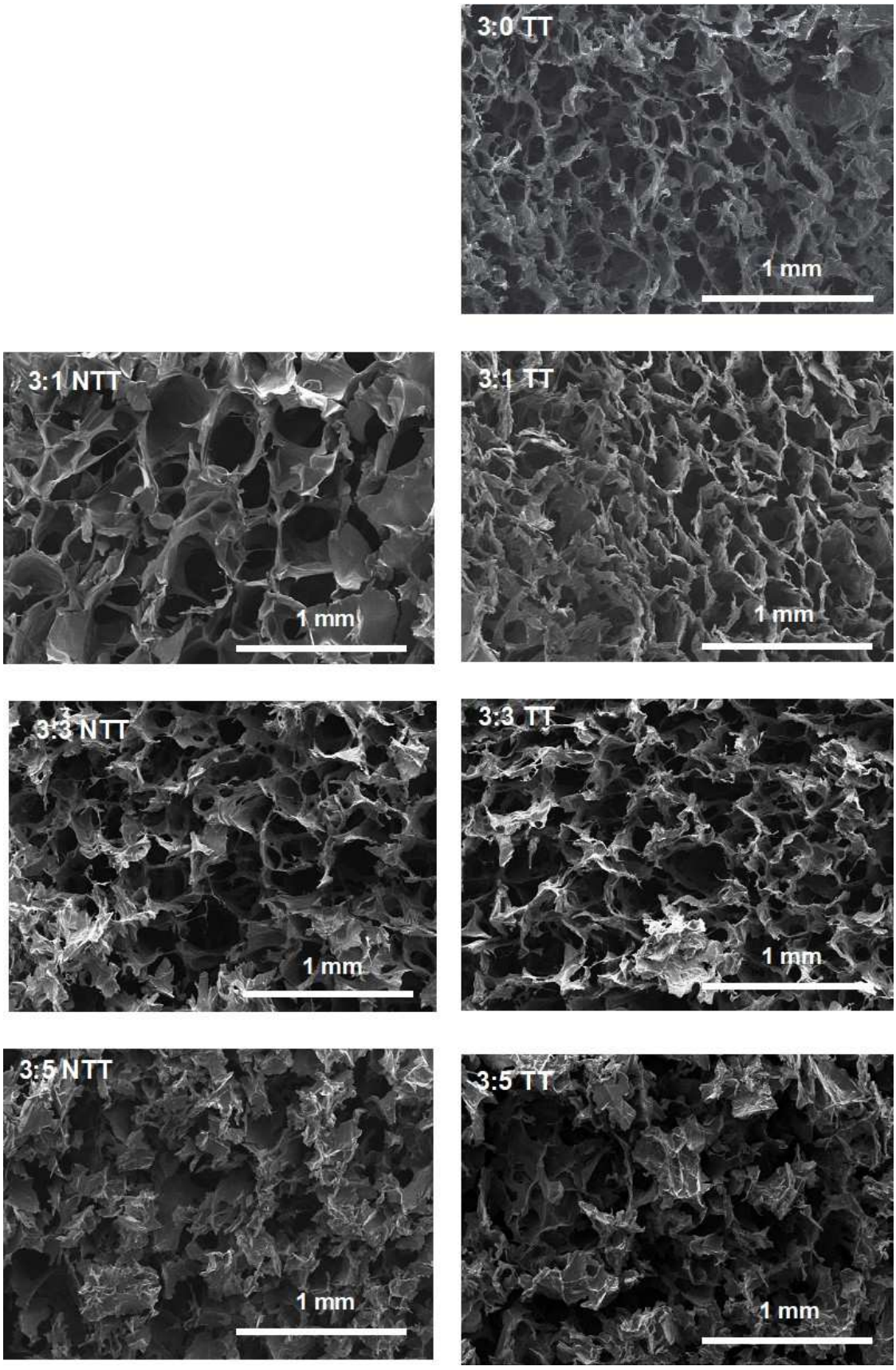

Figure 6 : SEM images of CHT:PCD 3:0 TT, 3:1 TT/NTT, 3:3 TT/NTT and 3:5 TT/NTT (magnification scale x50)

3.2.3 Sponge kinetics of degradation

Lysozyme was used for evaluating sponge stability as it is known to degrade CHT *in vivo* (Kean and Thanou, 2010)(Jennings, 2017)(Szymańska and Winnicka, 2015). It is also involved in the defence mechanisms against bacterial infections in vertebrates (Jennings, 2017)(Ibrahim et al., 1991). Degradation of CHT:PCD sponges were evaluated for 7 days (168 h) in PBS at 37 °C with (figure 7 C and D) and without lysozyme (figure 7 A and B).

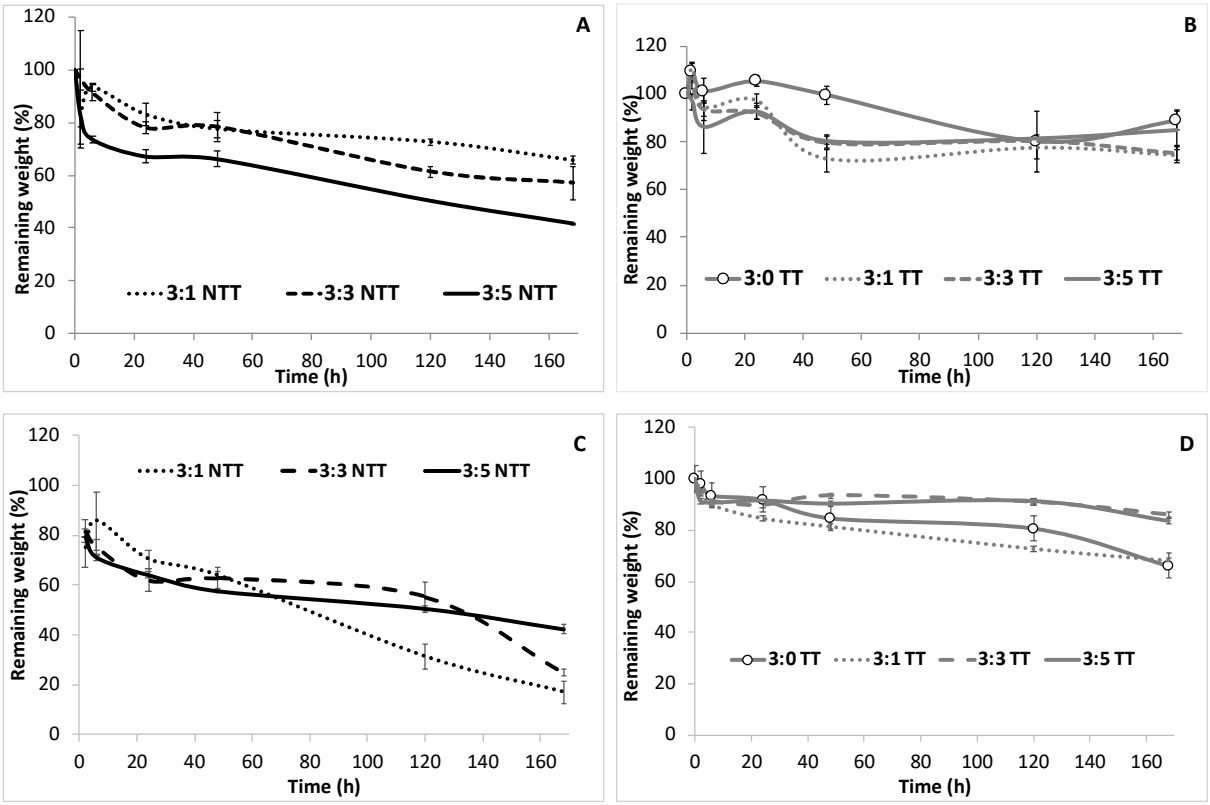

Figure 7 : Degradation profiles of CHT:PCD sponges NTT (A and C) and TT (B and D) in a PBS pH 7.4 (A and B) solution enriched with lysozyme (C and D) at 37°C under 80 rpm. Mean of N=3 samples

In the absence of lysozyme, degradation profiles showed a progressive sponge mass (in %) decrease over time. Thus, after 7 days, the mass loss observed in the 3:1 NTT, 3:3 NTT and 3:5 NTT sponges (figure 7 A) were 34 ± 2%, 43 ± 6% and 58 ± 0%, respectively. The degradation rate of the non-thermal treated systems is influenced by the PCD amount in the formulation. The larger this quantity is, the greater the mass loss is. This observation is the result of the PCD solubilisation in the PBS solution. After thermal treatment (figure 7 B), sponges showed a mass loss limited to 12-25 %, without any significant difference between ratios ($p < 0.05$). This is explained by the PCD crosslinking with CHT by amide (and ester) bond formations as described previously.

In the presence of lysozyme, degradation kinetics were accelerated, with the greater mass loss observed for non-thermal treated sponges, due to the action of lysozyme on CHT (figure 7 C and D). After 7 days, the mass loss for 3:1 NTT, 3:3 NTT and 3:5 NTT sponges was 83 ± 5%, 75 ± 1% and 58 ± 3% respectively. In contrast to what has been described above, sponge degradation is slower with the increase of PCD proportion in the formulation. The cross-linked polymer network prevents the diffusion and the enzyme activity. It is important to note that cross-linked sponges showed better stability over time than non-cross-linked sponges, either in the presence or the absence of lysozyme. The effect of heat treatment on the stability of CHT and PCD-based PECs has already been demonstrated in previous work from our team. Aubert-Viard et *al.* showed an improvement in the stability of their multi-layered system after heat treatment at 140°C (Aubert-Viard et al., 2019). Ji and Shi also reported that CHT sponges degraded more slowly after thermal crosslinking at 121 °C (Ji and Shi, 2013). Ouerghemmi *et al.* and more recently Kersani *et al.* also reported that electrospun nanofibers based on CHT and poly(cyclodextrin citrate) were also stabilised in aqueous medium after a thermal treatment (Ouerghemmi et al., 2016)(Kersani et al., 2020).

3.2.4. Swelling rate of sponges in PBS

In the clinical context, the device will often be applied in deep wounds. The sponge must swell after impregnation in the antibiotic solution to fill the cavity and to release antibacterial agents over the entire wound surface. Drug absorption and release are partly correlated to the swelling rate (Koetting et al., 2015)(Fatimi et al., 2009). It was therefore evaluated before (figure 8 A) and after thermal post-treatment (figure 8 B) at regular time intervals for 24 hours in a PBS solution at 37°C, 80 rpm as shown in figure 43.

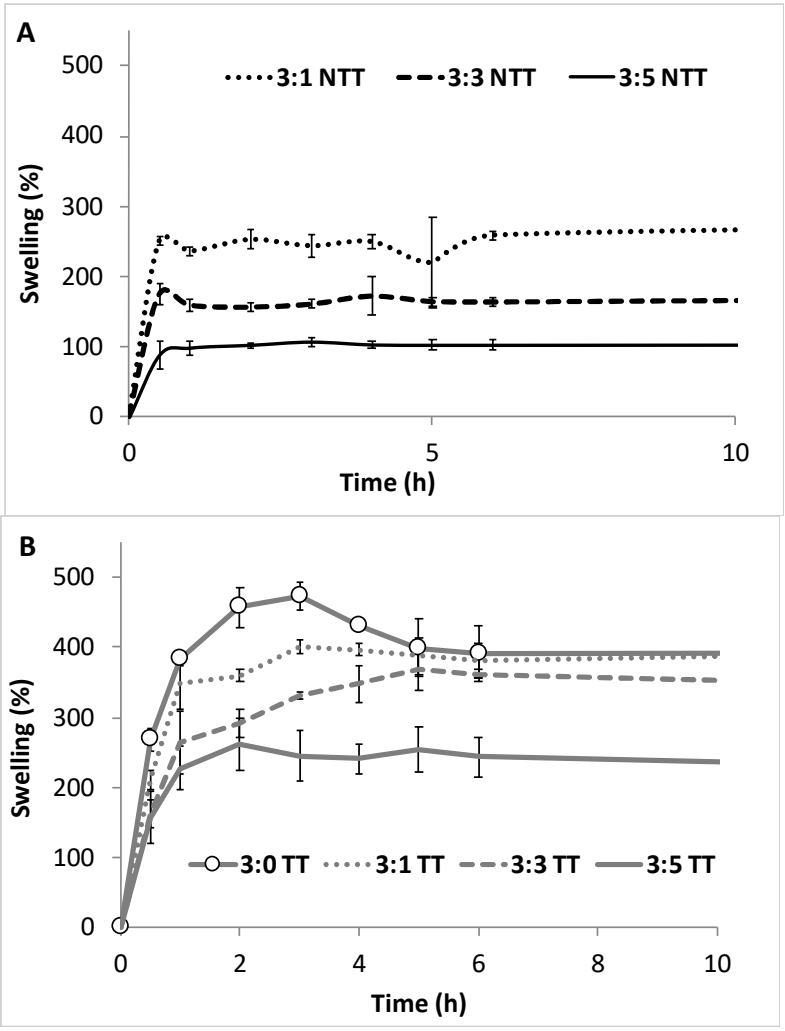

Figure 8 : Swelling profiles of CHT:PCD sponges NTT (A) and TT (B) after immersion in a PBS solution at 37 °C and 80 rpm. Mean of N=3 samples

The swelling of non-crosslinked sponges showed a profile with a very rapid increase during the first hour before reaching a plateau (236 ± 7%, 159 ± 10% and 98 ± 10% respectively for the ratios 3:1 NTT, 3:3 NTT and 3:5 NTT). A rapid swelling rate increase was also observed for the heat-treated sponges during the first hour, then the progression was slower and stabilised after 6 hours at 393 ± 40%, 382 ± 24%, 362 ± 6% and 244 ± 29% respectively for the ratios 3:0 TT, 3:1 TT, 3:3 TT and 3:5 TT. These swelling rates are influenced by two main parameters: 1). For the non-crosslinked sponges, the increase of PCD amount in the formulation leads to a decrease in the rate of swelling. The degradation study showed that the mass loss depends on the PCD proportion for these samples. The swelling rate is influenced by this loss of material. 2) On the other hand, the heat treatment induces the partial conversion of ionic interactions into amine bonds. Thus, the system is stabilised, and degradation slows down in an aqueous medium. The mass lost is then less significant, and the swelling is underestimated less, so is therefore more relevant for the cross-linked sponges. The

absorption capacity for these sponges decreases with the addition of PCD to the preparation because the crosslinking limits the swelling. The 3:0 TT formulation therefore swells the most. Although we observed different swelling rates, all sponges are able to absorb several times their own mass, displaying superabsorbent-like properties.

3.2.5. Mechanical properties of sponges

DFI wounds are large and deep lesions. The device must be able to be compressed for insertion and return to its original shape after expansion into the wound to fill the entire defect, without exerting too much deleterious pressure on the edges. After samples were rehydrated in a PBS solution for 4 h at 37 °C, 80 rpm, mechanical properties were assessed by applying a 50% deformation. Each sample showed similar strain-stress curves with two distinct regions (figure 9). The first cycle is the increase of stress during compression and the second is its decrease during the return of the piston to its initial position. It is important to note that no sponge displayed any fractures or ruptures under the 50% deformation.

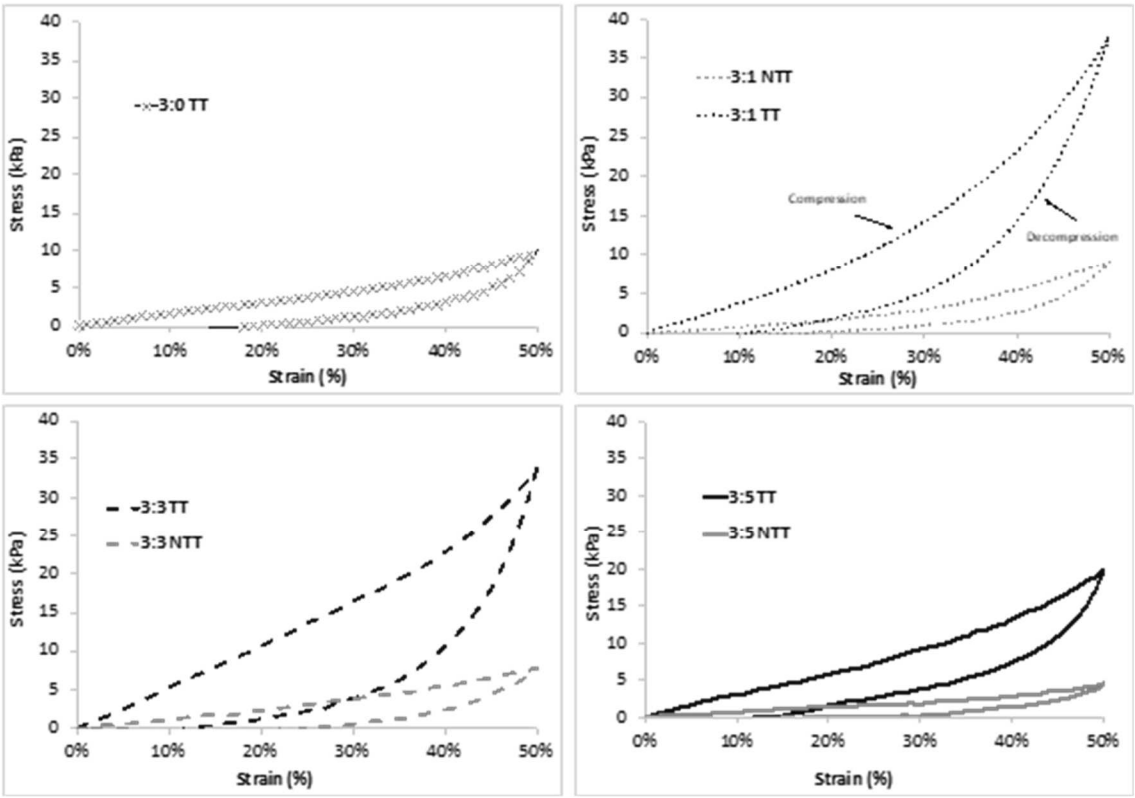

Figure 9 : Curves of compression and decompression as a function of the stress applied during the compression-decompression of sponges 3: 0 TT, 3: 1 NTT / TT, 3: 3 NTT / TT and 3: 5 NTT / TT. N = 3 samples

All materials were characterised by a compressive modulus or Young's modulus (E), which must be compatible with that of the surrounding tissues *in vivo*. This modulus was calculated from the linear region portion of the compression cycle. In addition, the residual deformation for each sponge was measured after the compression was released at 50% of the initial size. Results are displayed in figure 10.

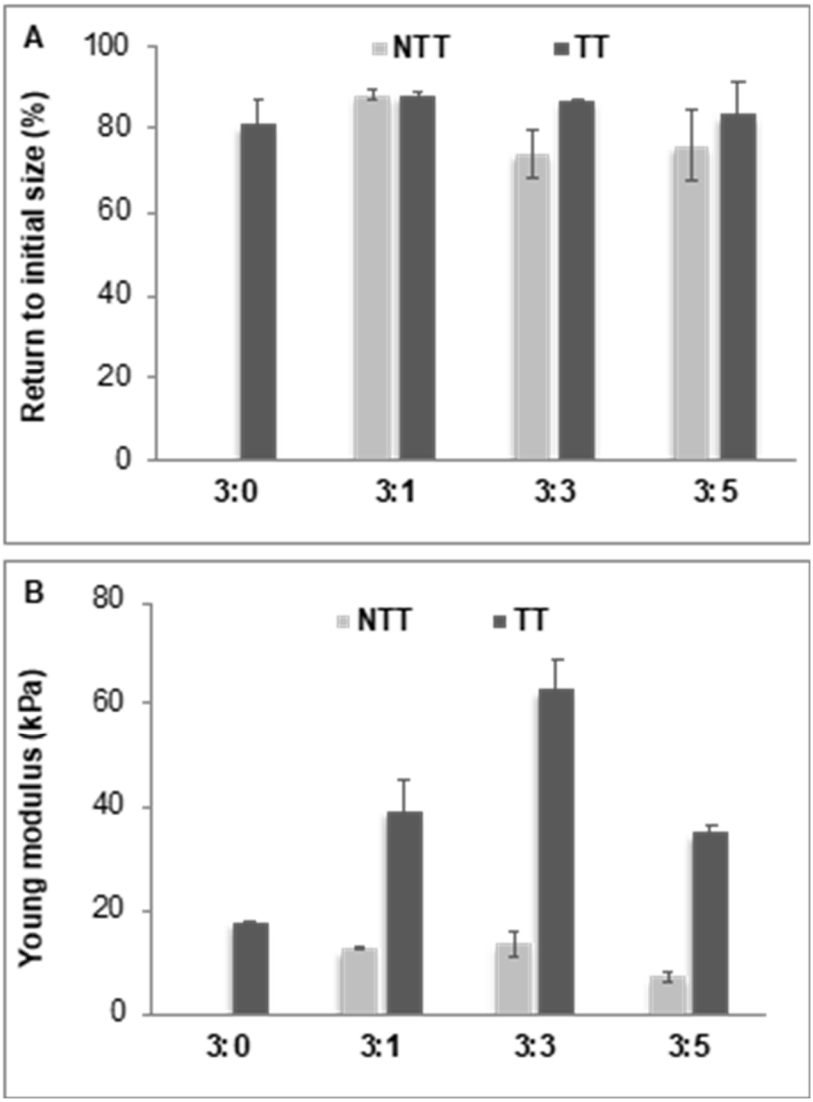

Figure 10 : (A) Evaluation of the percentage of return to initial shape after a 50 % compression for the sponges CHT:PCD NTT and TT; (B) Young 's modulus according to the ratio of sponges CHT:PCD NTT and TT. Mean of N=3 samples

After a 50 % compression, sponges presented a small irreversible deformation of approximately 20 % (88 ± 1 %, 74 ± 6 % and 76 ± 9 % respectively for ratios 3:1, 3:3 and 3:5 NTT, and 81 ± 7 %, 89 ± 1 %, 87 %, and 84 ± 7 % for formulations 3:0, 3:1, 3:3 and 3:5 TT), with no significant differences between samples ($p > 0.05$) (figure 9 A). After application, the sponges will expand again without exerting pressure on the defect edges but will not cover the entire wound volume. Plastic deformation due to

non-reversing phenomena occurring during the compression phase must therefore be taken into account when cutting the sponge with a recommended oversizing of 20 % (Kitahara et al., 2017)(Pernès, 2015). figure 9 B shows the evolution of Young's moduli depending on the CHT:PCD ratio before and after heat treatment. The non-crosslinked sponges, 3:1 NTT and 3:3 NTT, had identical moduli values of 13 kPa while the 3:5 NTT sponges presented a modulus of 7 kPa. After heat treatment, these values increased significantly. As the increase measured after thermal treatment was 3.1, 4.8 and 5.0 fold for 3:1, 3:3 and 3:5 ratios respectively. Furthermore, sponge values of Young's moduli after thermal treatment was obviously dependent on their ratio. Thus, Young's modulus increased from 13 ± 3 kPa for the 3:0 TT formulation up to 39 ± 6 kPa and 63 ± 6 kPa for ratios 3:1 and 3:3 TT and then decreased to 35 ± 1 kPa for the 3:5 TT formulation. As such, Young's modulus increase observed after thermal treatment is explained by the crosslinking through the formation of covalent bonds between PCD and CHT, resulting in an increase in the material's rigidity. In fact, the highest values of Young's moduli measured for the 3:3 sample are in perfect agreement with the rheological study aforementioned above that also displayed the highest storage modulus G' value of its precursor hydrogel formulation.

From rheological data, it appears that the 3:3 ratio corresponding to the molar ratio equals to 1.25 between the amine function of CHT and the PCD carboxylic acids (Table 2) is the best condition for providing the highest density in ionic crosslinks in the polymer network in its hydrogel form. The mechanical test clearly indicated that the same ratio is also the best compromise for the formation of dense amide crosslink bonding between carboxylic groups of PCD and ammonium groups of CHT, resulting in the highest Young's modulus of the freeze-dried material.

In addition, SEM analysis of 3:5 TT sponges showed a different microstructure from the other formulations. We observed a loss of porosity and therefore of the spongy microarchitecture with a thickening of the walls due to the PCD excess. This spongy microarchitecture allows the coalescence of the pores that protect the material during compression (Gibson and Ashby, 2001). Therefore, the structure of the 3:5 TT ratio leads to a decrease in compressive strength. The sponges will mainly be in contact with the skin which lies in the same range as the cross-linked sponges' Young's modulus, i.e. approximately 50 kPa (Xing Liang and Boppart, 2010). A sponge with a Young's modulus that is too low will show poor mechanical strength and may show deformities and in consequence will not fill the entire volume of the infected wound. On the other hand, a Young's modulus with a value that is too high will result in a stiff material that will apply too much pressure to the edge of the wound. The 3:1 TT, 3:3 TT and 3:5 TT sponges therefore have the most compatible mechanical properties with the clinical application we are targeting.

3.2.6. Cytotoxicity evaluation

Diabetic foot infections are often deep and affects the bone in the majority of cases. The CHT:PCD sponges are intended to be implanted in the lesion and will be in contact with damaged skin and bone needing cytotoxicity evaluation using pre-osteoblast cells.

The pre-osteoblast cell viability was 99 ± 15%, 74 ± 10% and 89 ± 16% in contact of extract from 3:1 NTT, 3:3 NTT and 3:5 NTT sponges respectively (figure 11). After thermal treatment, cell viability increased to 111 ± 9%, 111 ± 12%, 99 ± 10% and 87 ± 6% for 3:0 TT, 3:1 TT, 3:3 TT and 3:5 TT sponges. However, no significant differences can be concluded between sponges of the same group (TT vs NTT) and between sponges of the same ratio (3:0; 3:1; 3:3 and 3:5) ($p > 0.05$). Pre-osteoblast cells survival rates were higher than 70 % after 24 hours of contact with extract medium, so according to ISO 190993-5 sponges were not cytotoxic. The cytocompatibility of CHT and PCD based materials described in recent studies is confirmed (Ouerghemmi et al., 2016)(Flores et al., 2017).

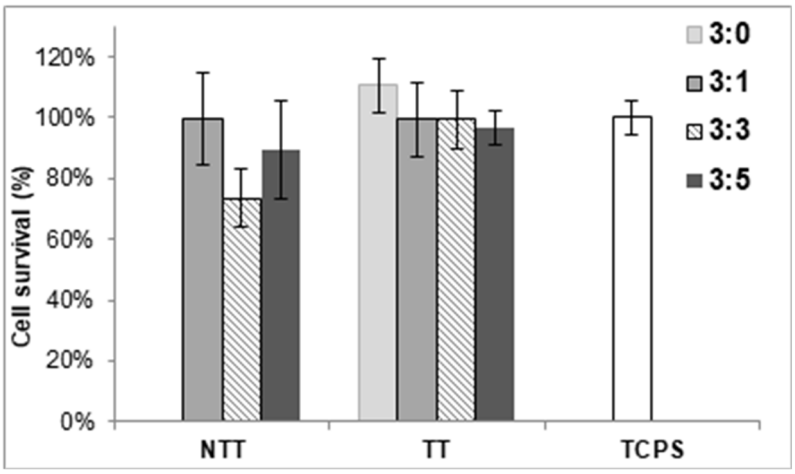

Figure 11 : Pre-osteoblast cells viability in presence of sponges extract medium after 24 hours of incubation compared to TCPS (Tissue culture polystyrene, negative control with absence of cytotoxicity). Extract medium was obtained after an incubation of sponges in culture medium during 24 hours (37°C,). Mean of N=18 samples

3.3. Ciprofloxacin release

The release media obtained after static release of CIP impregnated sponges were analysed by HPLC. Antibiotic discharges and kinetic profiles were obtained by UV dosage and are presented in figure 12.

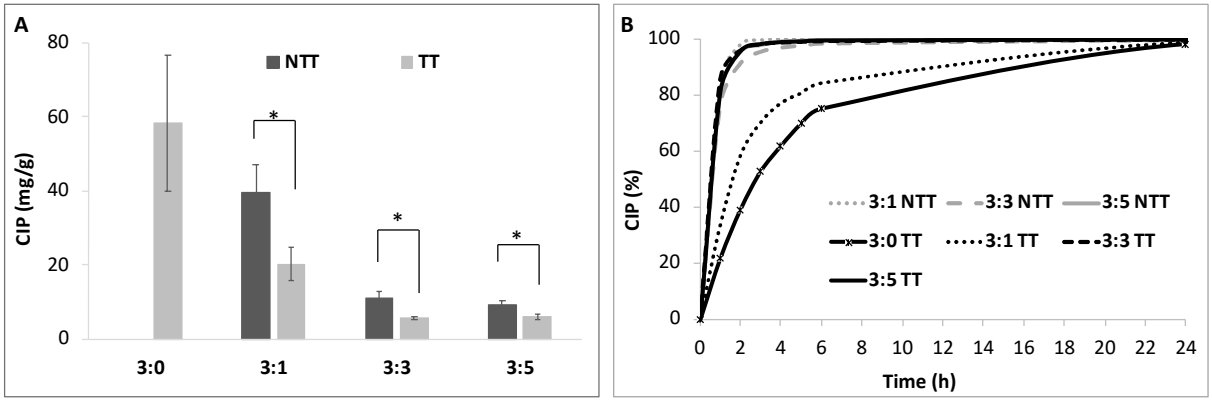

Figure 12 : (A) Ciprofloxacin sorption of sponges NTT (3:1, 3:3 and 3:5) and TT (3:0, 3:1, 3:3 and 3:5) (* statistic difference between groups for p < 0,005); (B) Kinetic profiles of sponge NTT (3:1, 3:3 and 3:5) and TT (3:0, 3:1, 3:3 and 3:5) under release in static condition during 24 hours at 37 °C and 80 rpm. Mean of n=6 samples

After 24 hours, sponges 3:0 TT delivered the highest CIP amount (58 ± 18 mg/g), as presented in figure 12 A. A decreased drug sorption was observed with a PCD increase in formulations. Ratio 3:1 NTT (40 ± 8 mg/g) released four times more than ratios 3:3 and 3:5 NTT (11 ± 2 mg/g and 10 ± 1 mg/g). Thermal treatment also had an influence on the drug release. A significant difference (p < 0,05) of quantity released was observed between sponges of the same ratio with and without thermal treatment. Release was greater when devices were not heat treated. As an example, sponges 3:1 NTT (40 ± 8 mg/g) released 2 times more CIP than ratio 3:1 TT (20 ± 4 mg/g). This observation may be related to the different types of interactions between CHT and PCD when the system is thermally treated or not. The NTT samples present pure PEC characteristics, while TT samples present PEC and covalent characteristics. Therefore, NTT samples display a higher density of ionic groups than TT samples, which are available for interacting with the carboxylate groups of CIP.

Kinetic release patterns (figure 12 B) showed a profile with an initial burst followed by a plateau. Sponges 3:1 NTT, 3:3 NTT/TT and 3:5 NTT/TT released more than 80 % of the antibiotic in 1 h and reached their plateau after 4h30. 3:1 TT and 3:0 TT kinetic releases were slower. 80 % of CIP was released in 5 h and 10 h respectively for these ratios and their plateau was reached after 24 h. Release profiles tend to be slower in formulations containing little or no PCD. These results are surprising as they do not show the expected effects of CDs on sustaining CIP release. Recently Aytac et *al.*, developed gelatin and β-CD nanofibers including CIP by its piperazin group (Aytac et al., 2019). This inclusion complex was also highlighted by Masoumi et *al*., made from polycaprolactone and CD nanofibers loaded with CIP (Masoumi et al., 2018). In our laboratory, we worked on materials functionalised with PCD for a sustained antibiotic release (Hoang Thi et al., 2010)(Leprêtre et al., 2009). 3:0 TT sponges showed the highest sorption with an extended kinetic release profile. A

correlation between swelling degree and sorption can be concluded. Sponges with a greater swelling rate *i.e.* 3:0 TT, absorb and release the highest dose of drugs with a slow sustained kinetic profile. Moreover, an interaction between CIP and CHT can be assumed. Fluoroquinolone, like CIP, are known to be a zwitterion at physiologic pH (Kamberi et al., 1999)(Blanco-Fernandez et al., 2011). The negative charge is carried by the carboxylate group COO^- and the positive charge is present on the piperazynil group. Inclusion complex CD-CIP is mainly due to dipole, hydrophobic interactions, and Van der Waal's forces (Jianbin et al., 2002). However, in our polyelectrolytes complex system, ionic bonds may contribute to a larger extent than inclusion complexation with CIP, therefore, carboxylate groups of PCD may compete with those of CIP toward CHT ammonium groups. This explains why the sponge absorbs less when there is a higher amount of PCD.

3.4. Antibacterial assay

To determine CIP sponges' antibacterial potential, a diffusion test (Kirby Bauer) was performed. After a static release in PBS, at different times, release media were collected and introduced in wells formed in MHA agar, previously seeded with bacteria. If the release medium shows an antibacterial activity, inhibition circles (inhibition of bacterial proliferation) were formed (after an incubation of 24 h at 37 °C) around the deposition site. The diameter of the circles are proportional to the amount of CIP released into the medium. We decided to test the impregnated samples on two references, *S. aureus* and *E. coli* strains, Gram+ and Gram- bacteria that is often isolated in DFIs. Results are presented figure 13 A and C for non-thermal treated sponges on *S. aureus* and *E. coli* respectively, and figure 13 B and D for thermal treated sponges.

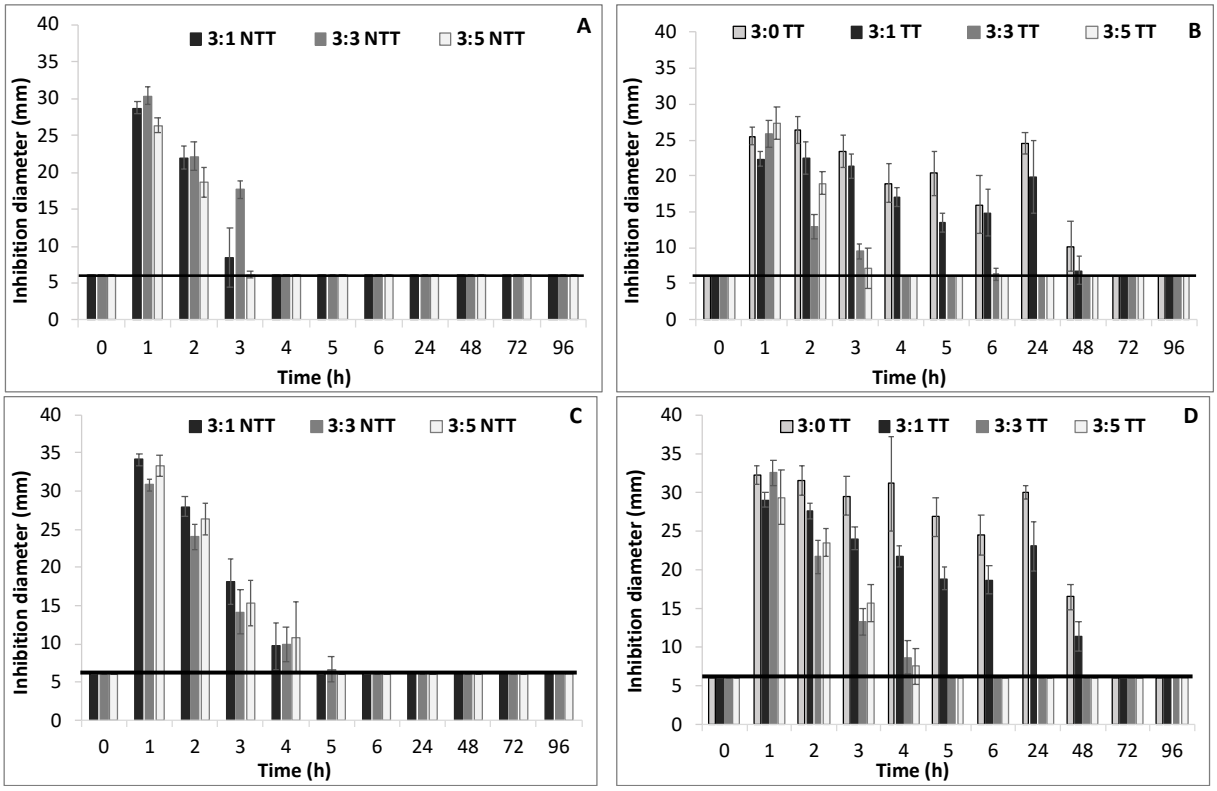

Figure 13 : (A) inhibition diameter (Kirby Bauer test) after static release on *Staphylococcus aureus* for NTT sponges (3:1, 3:3 and 3:5); (B) Kirby Bauer test on *Staphylococcus aureus* for TT sponges (3:0, 3:1, 3:3 and 3:5); (C) Kirby Bauer test on *Escherichia coli* for NTT sponges (3:1, 3:3 and 3:5); (D) Kirby Bauer test on *Escherichia coli* for TT sponges (3:0, 3:1, 3:3 and 3:5). Mean of n=6 samples

Figure 13 shows that the antibacterial activity of the release media decreases over time regardless of the strain and sample tested. Inhibition circles were observed until 3 h and 4 h for non-crosslinked sponges, respectively on *S. aureus* (figure 13 A) and *E. coli* (figure 13 C). Ratios 3:3 and 3:5 showed a similar activity with or without thermal treatment. On the other hand, the antibacterial activity was improved for sponges 3:1 after thermal cross-linking. Inhibition circles were still visible at 48 h on *S. aureus* (figure 13 B) and *E. coli* (figure 13 D). Control sponges 3:0 TT also had an extended inhibition of 48 h but slightly more important in terms of diameter size than 3:1 TT samples. For example, at 24 h of release, the inhibition diameters were 25 ± 2 mm and 20 ± 5 mm for the 3:0 TT and 3:1 TT samples on *S. aureus* and 30 ± 1 mm and 23 ± 3 mm on *E. coli*. These observations suggest that there is a correlation between the amount of drug absorbed and the bacterial inhibition profile. Absorption capacity and antibacterial activity are the most important for the 3:0 TT ratio. Sponge loadings, therefore, seem to have an influence on the antibiotic release profiles and the duration of its antibacterial activity.

It is important to note that a more sustained activity on *E. coli* than *S. aureus* was observed. We found that Gram- are more susceptible to CIP than Gram+ (Ali et al., 2010). This difference in

susceptibility mainly depends on the molecule's ability to penetrate the bacterial wall before acting within cell cytoplasm (Wehrli, 1983). Studies showed a correlation between the hydrophobic/hydrophilic characteristics of a molecule and its penetration through the bacteria. CIP accumulation analysis in *E. coli* demonstrated a better diffusion of hydrophilic molecules through its membrane (Bazile et al., 1992). It has been recognised that the less hydrophobic a compound is, the better the penetration is (Nikaido et al., 1983).

3.5. Conclusion

For our first approach, CHT:PCD based hydrogels with different CHT:PCD weight ratios were prepared. Rheological tests showed that the 3:3 ratio presented the optimal ionic crosslink density that yields hydrogels with the most elastic characteristics. This was due to the optimal balance between carboxylic groups and amino groups and as a consequence produced the highest ionic crosslink density in the CHT:PCD network. Sponges were obtained from freeze drying the CHT:PCD hydrogels. SEM images did not reveal microarchitecture differences before and after thermal treatment. However, the alveolar microstructure was affected upon PCD increase in the formulation.

Our results concluded that CIP absorption/release decreased with increasing PCD ratio in sponge formulations. CIP is shown to interact with CHT:PCD system by inclusion complexation with CD cavities, however due to its zwitterion character, CIP interacts to a larger extent through ionic interactions with the CHT:PCD system. In addition, applying a thermal post-treatment increased the mechanical properties of the sponges, reduced their degradation rate, and increased the swelling of the sponges, but decreased their sorption capacity toward CIP by reducing the available ionic groups in the system. The diffusion test confirmed the release kinetic tests, highlighting the best antibacterial performances of ratios 3:0 TT and 3:1 TT, suggesting a correlation between the amount of antibiotics absorbed by the sponge and the antibacterial profile.

To conclude, more tests need to be conducted, especially microbiology and *in vivo* experiments to define the best compromise between the beneficial effect of PCD on the mechanical properties of the sponges, and on their stability in aqueous medium versus its unexpected negative effects on the sorption/release properties toward CIP. However, the next studies will need to investigate the behaviour of our CHT:PCD system on other types of antibiotics efficient in diabetic foot infections than CIP, and which would not present the aforementioned zwiterionic characteristics.

Acknowledgments

This research was supported by FONDECYT-CONCYTEC (grant contract number 274-2015-FONDECYT) and ArCiR Program (BIOCERMED)

Ali, S.Q., Zehra, A., Naqvi, B.S., Shah, S., Bushra, R., 2010. Resistance Pattern of Ciprofloxacin Against Different Pathogens. Oman Med. J. 25, 294–298. https://doi.org/10.5001/omj.2010.85

Anraku, M., Iohara, D., Hiraga, A., Uekama, K., Ifuku, S., Pipkin, J.D., Hirayama, F., 2015. Formation of Elastic Gels from Deacetylated Chitin Nanofibers Reinforced with Sulfobutyl Ether β-Cyclodextrin. Chem. Lett. 44, 285–287. https://doi.org/10.1246/cl.141004

Arslan, M., Yirmibesoglu, T., Celebi, M., 2018. In situ Crosslinkable Thiol-ene Hydrogels Based on PEGylated Chitosan and β-Cyclodextrin. J. Turk. Chem. Soc. Sect. Chem. 1327–1336. https://doi.org/10.18596/jotcsa.460275

Aubert-Viard, F., Mogrovejo-Valdivia, A., Tabary, N., Maton, M., Chai, F., Neut, C., Martel, B., Blanchemain, N., 2019. Evaluation of antibacterial textile covered by layer-by-layer coating and loaded with chlorhexidine for wound dressing application. Mater. Sci. Eng. C 100, 554–563. https://doi.org/10.1016/j.msec.2019.03.044

Aytac, Z., Ipek, S., Erol, I., Durgun, E., Uyar, T., 2019. Fast-dissolving electrospun gelatin nanofibers encapsulating ciprofloxacin/cyclodextrin inclusion complex. Colloids Surf. B Biointerfaces 178, 129–136. https://doi.org/10.1016/j.colsurfb.2019.02.059

Bazile, S., Moreau, N., Bouzard, D., Essiz, M., 1992. Relationships among antibacterial activity, inhibition of DNA gyrase, and intracellular accumulation of 11 fluoroquinolones. Antimicrob. Agents Chemother. 36, 2622–2627. https://doi.org/10.1128/AAC.36.12.2622

Blanchemain, N., Martel, B., Flores, C., Cazaux, F., Chai, F., Tabary, N., 2017. Method for the Production of Hydrogel Comprising Chitosan and Negatively Charged Polyelectrolytes, and Cellular, Porous Material Resulting from Said Hydrogel. FR3038318 (A1).

Blanco-Fernandez, B., Lopez-Viota, M., Concheiro, A., Alvarez-Lorenzo, C., 2011. Synergistic performance of cyclodextrin–agar hydrogels for ciprofloxacin delivery and antimicrobial effect. Carbohydr. Polym. 85, 765–774. https://doi.org/10.1016/j.carbpol.2011.03.042

Borzacchiello, A., Ambrosio, L., 2009. Structure-Property Relationships in Hydrogels, in: Hydrogels. Springer Milan, Milano, pp. 9–20. https://doi.org/10.1007/978-88-470-1104-5_2

Costa Almeida, C.E., 2016. Collagen implant with gentamicin sulphate as an option to treat a neuroischaemic diabetic foot ulcer: Case report. Int. J. Surg. Case Rep. 21, 48–51. https://doi.org/10.1016/j.ijscr.2016.02.023

Endogan Tanir, T., Hasirci, V., Hasirci, N., 2015. Preparation and characterization of Chitosan and PLGA-based scaffolds for tissue engineering applications. Polym. Compos. 36, 1917–1930. https://doi.org/10.1002/pc.23100

Fatimi, A., Tassin, J.-F., Turczyn, R., Axelos, M.A.V., Weiss, P., 2009. Gelation studies of a cellulose-based biohydrogel: The influence of pH, temperature and sterilization. Acta Biomater. 5, 3423–3432. https://doi.org/10.1016/j.actbio.2009.05.030

Flores, C., Lopez, M., Tabary, N., Neut, C., Chai, F., Betbeder, D., Herkt, C., Cazaux, F., Gaucher, V., Martel, B., Blanchemain, N., 2017. Preparation and characterization of novel chitosan and β-cyclodextrin polymer sponges for wound dressing applications. Carbohydr. Polym. 173, 535–546. https://doi.org/10.1016/j.carbpol.2017.06.026

Garcia-Fernandez, M.J., Tabary, N., Chai, F., Cazaux, F., Blanchemain, N., Flament, M.-P., Martel, B., 2016. New multifunctional pharmaceutical excipient in tablet formulation based on citric acid-cyclodextrin polymer. Int. J. Pharm. 511, 913–920. https://doi.org/10.1016/j.ijpharm.2016.07.059

Gauland, C., 2011. Managing Lower-Extremity Osteomyelitis Locally with Surgical Debridement and Synthetic Calcium Sulfate Antibiotic Tablets: Adv. Skin Wound Care 24, 515–523. https://doi.org/10.1097/01.ASW.0000407647.12832.6c

Gibson, L.J., Ashby, M.F., 2001. Cellular solids: structure and properties, 2. ed., 1. paperback ed. (with corr.), transferred to digital printing. ed, Cambridge solid state science series. Cambridge Univ. Press, Cambridge.

Herbois, R., Noël, S., Léger, B., Tilloy, S., Menuel, S., Addad, A., Martel, B., Ponchel, A., Monflier, E., 2015. Ruthenium-containing β-cyclodextrin polymer globules for the catalytic hydrogenation of biomass-derived furanic compounds. Green Chem. 17, 2444–2454. https://doi.org/10.1039/C5GC00005J

Hoang Thi, T.H., Chai, F., Leprêtre, S., Blanchemain, N., Martel, B., Siepmann, F., Hildebrand, H.F., Siepmann, J., Flament, M.P., 2010. Bone implants modified with cyclodextrin: Study of drug release in bulk fluid and into agarose gel. Int. J. Pharm. 400, 74–85. https://doi.org/10.1016/j.ijpharm.2010.08.035

Ibrahim, H.R., Kato, A., Kobayashi, K., 1991. Antimicrobial effects of lysozyme against gram-negative bacteria due to covalent binding of palmitic acid. J. Agric. Food Chem. 39, 2077–2082. https://doi.org/10.1021/jf00011a039

Jennings, J. A., 2017. 7 - Controlling chitosan degradation properties in vitro and in vivo, in: Jennings, J. Amber, Bumgardner, J.D. (Eds.), Chitosan Based Biomaterials Volume 1. Woodhead Publishing, pp. 159–182. https://doi.org/10.1016/B978-0-08-100230-8.00007-8

Ji, C., Shi, J., 2013. Thermal-crosslinked porous chitosan scaffolds for soft tissue engineering applications. Mater. Sci. Eng. C 33, 3780–3785. https://doi.org/10.1016/j.msec.2013.05.010

Jianbin, C., Liang, C., Hao, X., Dongpin, M., 2002. Preparation and study on the solid inclusion complex of ciprofloxacin with β-cyclodextrin. Spectrochim. Acta. A. Mol. Biomol. Spectrosc. 58, 2809–2815. https://doi.org/10.1016/S1386-1425(02)00078-1

Jin, R., Moreira Teixeira, L.S., Dijkstra, P.J., Karperien, M., van Blitterswijk, C.A., Zhong, Z.Y., Feijen, J., 2009. Injectable chitosan-based hydrogels for cartilage tissue engineering. Biomaterials 30, 2544–2551. https://doi.org/10.1016/j.biomaterials.2009.01.020

Kamberi, M., Tsutsumi, K., Kotegawa, T., Kawano, K., Nakamura, K., Niki, Y., Nakano, S., 1999. Influences of Urinary pH on Ciprofloxacin Pharmacokinetics in Humans and Antimicrobial Activity In Vitro versus Those of Sparfloxacin. Antimicrob. Agents Chemother. 43, 525–529.

Karr, J.C., 2011. Management in the Wound-care Center Outpatient Setting of a Diabetic Patient with Forefoot Osteomyelitis Using Cerament Bone Void Filler Impregnated with Vancomycin: Off-label Use. J. Am. Podiatr. Med. Assoc. 101, 259–264. https://doi.org/10.7547/1010259

Kean, T., Thanou, M., 2010. Biodegradation, biodistribution and toxicity of chitosan. Adv. Drug Deliv. Rev. 62, 3–11. https://doi.org/10.1016/j.addr.2009.09.004

Kersani, D., Mougin, J., Lopez, M., Degoutin, S., Tabary, N., Cazaux, F., Janus, L., Maton, M., Chai, F., Sobocinski, J., Blanchemain, N., Martel, B., 2020. Stent coating by electrospinning with chitosan/poly-cyclodextrin based nanofibers loaded with simvastatin for restenosis prevention. Eur. J. Pharm. Biopharm. 150, 156–167. https://doi.org/10.1016/j.ejpb.2019.12.017

Kitahara, H., Okada, K., Kimura, T., Yock, P.G., Lansky, A.J., Popma, J.J., Yeung, A.C., Fitzgerald, P.J., Honda, Y., 2017. Impact of Stent Size Selection on Acute and Long-Term Outcomes After Drug-Eluting Stent Implantation in De Novo Coronary Lesions. Circ. Cardiovasc. Interv. 10. https://doi.org/10.1161/CIRCINTERVENTIONS.116.004795

Koetting, M.C., Peters, J.T., Steichen, S.D., Peppas, N.A., 2015. Stimulus-responsive hydrogels: Theory, modern advances, and applications. Mater. Sci. Eng. R Rep. 93, 1–49. https://doi.org/10.1016/j.mser.2015.04.001

Kong, M., Chen, X.G., Xing, K., Park, H.J., 2010. Antimicrobial properties of chitosan and mode of action: A state of the art review. Int. J. Food Microbiol. 144, 51–63. https://doi.org/10.1016/j.ijfoodmicro.2010.09.012

Leprêtre, S., Chai, F., Hornez, J.-C., Vermet, G., Neut, C., Descamps, M., Hildebrand, H.F., Martel, B., 2009. Prolonged local antibiotics delivery from hydroxyapatite functionalised with cyclodextrin polymers. Biomaterials 30, 6086–6093. https://doi.org/10.1016/j.biomaterials.2009.07.045

Li, J., Mooney, D.J., 2016. Designing hydrogels for controlled drug delivery. Nat. Rev. Mater. 1. https://doi.org/10.1038/natrevmats.2016.71

Li, L., Yu, F., Zheng, L., Wang, R., Yan, W., Wang, Z., Xu, J., Wu, J., Shi, D., Zhu, L., Wang, X., Jiang, Q., 2019. Natural hydrogels for cartilage regeneration: Modification, preparation and application. J. Orthop. Transl. 17, 26–41. https://doi.org/10.1016/j.jot.2018.09.003

Lipsky, B.A., Aragón-Sánchez, J., Diggle, M., Embil, J., Kono, S., Lavery, L., Senneville, É., Urbančič-Rovan, V., Van Asten, S., Peters, E.J.G., on behalf of the International Working Group on the Diabetic Foot (IWGDF), 2016. IWGDF guidance on the diagnosis and management of foot infections in persons with diabetes: IWGDF Guidance on Foot Infections. Diabetes Metab. Res. Rev. 32, 45–74. https://doi.org/10.1002/dmrr.2699

Loftsson, T., Jarho, P., Másson, M., Järvinen, T., 2005. Cyclodextrins in drug delivery. Expert Opin. Drug Deliv. 2, 335–351. https://doi.org/10.1517/17425247.2.1.335

Luo, Y., Wang, Q., 2014. Recent development of chitosan-based polyelectrolyte complexes with natural polysaccharides for drug delivery. Int. J. Biol. Macromol. 64, 353–367. https://doi.org/10.1016/j.ijbiomac.2013.12.017

Machín, R., Isasi, J.R., Vélaz, I., 2012. β-Cyclodextrin hydrogels as potential drug delivery systems. Carbohydr. Polym. 87, 2024–2030. https://doi.org/10.1016/j.carbpol.2011.10.024

Martel, B., Ruffin, D., Weltrowski, M., Lekchiri, Y., Morcellet, M., 2005. Water-soluble polymers and gels from the polycondensation between cyclodextrins and poly(carboxylic acid)s: A study of the preparation parameters. J. Appl. Polym. Sci. 97, 433–442. https://doi.org/10.1002/app.21391

Martin, A., Tabary, N., Leclercq, L., Junthip, J., Degoutin, S., Aubert-Viard, F., Cazaux, F., Lyskawa, J., Janus, L., Bria, M., Martel, B., 2013a. Multilayered textile coating based on a β-cyclodextrin polyelectrolyte for the controlled release of drugs. Carbohydr. Polym. 93, 718–730.

https://doi.org/10.1016/j.carbpol.2012.12.055

Martin, A., Tabary, N., Leclercq, L., Junthip, J., Degoutin, S., Aubert-Viard, F., Cazaux, F., Lyskawa, J., Janus, L., Bria, M., Martel, B., 2013b. Multilayered textile coating based on a β-cyclodextrin polyelectrolyte for the controlled release of drugs. Carbohydr. Polym. 93, 718–730. https://doi.org/10.1016/j.carbpol.2012.12.055

Masoumi, S., Amiri, S., Bahrami, S.H., 2018. PCL-based nanofibers loaded with ciprofloxacin/cyclodextrin containers. J. Text. Inst. 109, 1044–1053. https://doi.org/10.1080/00405000.2017.1398625

Matsumine, H., Fujimaki, H., Takagi, M., Mori, S., Iwata, T., Shimizu, M., Takeuchi, M., 2019. Full-thickness skin reconstruction with basic fibroblast growth factor-impregnated collagen-gelatin sponge. Regen. Ther. 11, 81–87. https://doi.org/10.1016/j.reth.2019.06.001

Mittal, H., Ray, S.S., Kaith, B.S., Bhatia, J.K., Sukriti, Sharma, J., Alhassan, S.M., 2018. Recent progress in the structural modification of chitosan for applications in diversified biomedical fields. Eur. Polym. J. 109, 402–434. https://doi.org/10.1016/j.eurpolymj.2018.10.013

Monnaert, V., Betbeder, D., Fenart, L., Bricout, H., Lenfant, A.M., Landry, C., Cecchelli, R., Monflier, E., Tilloy, S., 2004. Effects of γ- and Hydroxypropyl-γ-cyclodextrins on the Transport of Doxorubicin across an in Vitro Model of Blood-Brain Barrier. J. Pharmacol. Exp. Ther. 311, 1115–1120. https://doi.org/10.1124/jpet.104.071845

Morley, R., Lopez, F., Webb, F., 2016. Calcium sulphate as a drug delivery system in a deep diabetic foot infection. The Foot 27, 36–40. https://doi.org/10.1016/j.foot.2015.07.002

Moura, L.I.F., Dias, A.M.A., Carvalho, E., de Sousa, H.C., 2013. Recent advances on the development of wound dressings for diabetic foot ulcer treatment—A review. Acta Biomater. 9, 7093–7114. https://doi.org/10.1016/j.actbio.2013.03.033

Moura, M.J., Faneca, H., Lima, M.P., Gil, M.H., Figueiredo, M.M., 2011. In Situ Forming Chitosan Hydrogels Prepared via Ionic/Covalent Co-Cross-Linking. Biomacromolecules 12, 3275–3284. https://doi.org/10.1021/bm200731x

Nikaido, H., Rosenberg, E.Y., Foulds, J., 1983. Porin channels in Escherichia coli: studies with beta-lactams in intact cells. J. Bacteriol. 153, 232–240.

Noel, S.P., Courtney, H.S., Bumgardner, J.D., Haggard, W.O., 2010. Chitosan Sponges to Locally Deliver Amikacin and Vancomycin: A Pilot In Vitro Evaluation. Clin. Orthop. Relat. Res. 468, 2074–2080. https://doi.org/10.1007/s11999-010-1324-6

Ouerghemmi, S., Degoutin, S., Tabary, N., Cazaux, F., Maton, M., Gaucher, V., Janus, L., Neut, C., Chai, F., Blanchemain, N., Martel, B., 2016. Triclosan loaded electrospun nanofibers based on a cyclodextrin polymer and chitosan polyelectrolyte complex. Int. J. Pharm. 513, 483–495. https://doi.org/10.1016/j.ijpharm.2016.09.060

Palomino-Durand, C., Lopez, M., Cazaux, F., Martel, B., Blanchemain, N., Chai, F., 2019. Influence of the Soluble–Insoluble Ratios of Cyclodextrins Polymers on the Viscoelastic Properties of Injectable Chitosan–Based Hydrogels for Biomedical Application. Polymers 11, 214. https://doi.org/10.3390/polym11020214

Pérez-Anes, A., Gargouri, M., Laure, W., Van Den Berghe, H., Courcot, E., Sobocinski, J., Tabary, N., Chai, F., Blach, J.-F., Addad, A., Woisel, P., Douroumis, D., Martel, B., Blanchemain, N., Lyskawa, J., 2015. Bioinspired Titanium Drug Eluting Platforms Based on a Poly-β-cyclodextrin–Chitosan Layer-by-Layer Self-Assembly Targeting Infections. ACS Appl. Mater. Interfaces 7, 12882–12893. https://doi.org/10.1021/acsami.5b02402

Pernès, J.-M., 2015. Les stents traditionnels modernes : de nouveaux concepts. J. Mal. Vasc. 40, 92–93. https://doi.org/10.1016/j.jmv.2014.12.107

Raghavan, S.R., Cipriano, B.H., 2006. Gel Formation: Phase Diagrams Using Tabletop Rheology and Calorimetry, in: Weiss, R.G., Terech, P. (Eds.), Molecular Gels: Materials with Self-Assembled Fibrillar Networks. Springer Netherlands, Dordrecht, pp. 241–252. https://doi.org/10.1007/1-4020-3689-2_9

Ramli, M., Tabassi, A.A., Hoe, K.W., 2013. Porosity, pore structure and water absorption of polymer-modified mortars: An experimental study under different curing conditions. Compos. Part B Eng. 55, 221–233. https://doi.org/10.1016/j.compositesb.2013.06.022

Roeder, B., Van Gils, C.C., Maling, S., 2000. Antibiotic beads in the treatment of diabetic pedal osteomyelitis. J. Foot Ankle Surg. 39, 124–130. https://doi.org/10.1016/S1067-2516(00)80037-X

Rogina, A., Ressler, A., Matić, I., Gallego Ferrer, G., Marijanović, I., Ivanković, M., Ivanković, H., 2017. Cellular hydrogels based on pH-responsive chitosan-hydroxyapatite system. Carbohydr. Polym. 166, 173–182. https://doi.org/10.1016/j.carbpol.2017.02.105

Roy, J.C., Salaün, F., Giraud, S., Ferri, A., Chen, G., Guan, J., 2017. Solubility of Chitin: Solvents, Solution Behaviors and Their Related Mechanisms, in: Xu, Z. (Ed.), Solubility of Polysaccharides. InTech. https://doi.org/10.5772/intechopen.71385

Stinner, D.J., Noel, S.P., Haggard, W.O., Watson, J.T., Wenke, J.C., 2010. Local antibiotic delivery using tailorable chitosan sponges: the future of infection control? J. Orthop. Trauma 24, 592–597. https://doi.org/10.1097/BOT.0b013e3181ed296c

Szymańska, E., Winnicka, K., 2015. Stability of Chitosan—A Challenge for Pharmaceutical and Biomedical Applications. Mar. Drugs 13, 1819–1846. https://doi.org/10.3390/md13041819

Uçkay, I., Aragón-Sánchez, J., Lew, D., Lipsky, B.A., 2015. Diabetic foot infections: what have we learned in the last 30 years? Int. J. Infect. Dis. 40, 81–91. https://doi.org/10.1016/j.ijid.2015.09.023

Uçkay, I., Kressmann, B., Di Tommaso, S., Portela, M., Alwan, H., Vuagnat, H., Maître, S., Paoli, C., Lipsky, B.A., 2018a. A randomized controlled trial of the safety and efficacy of a topical gentamicin–collagen sponge in diabetic patients with a mild foot ulcer infection. SAGE Open Med. 6, 205031211877395. https://doi.org/10.1177/2050312118773950

Uçkay, I., Kressmann, B., Malacarne, S., Toumanova, A., Jaafar, J., Lew, D., Lipsky, B.A., 2018b. A randomized, controlled study to investigate the efficacy and safety of a topical gentamicin-collagen sponge in combination with systemic antibiotic therapy in diabetic patients with a moderate or severe foot ulcer infection. BMC Infect. Dis. 18. https://doi.org/10.1186/s12879-018-3253-z

van de Manakker, F., Vermonden, T., van Nostrum, C.F., Hennink, W.E., 2009. Cyclodextrin-Based Polymeric Materials: Synthesis, Properties, and Pharmaceutical/Biomedical Applications. Biomacromolecules 10, 3157–3175. https://doi.org/10.1021/bm901065f

Volmer-Thole, M., Lobmann, R., 2016. Neuropathy and Diabetic Foot Syndrome. Int. J. Mol. Sci. 17, 917. https://doi.org/10.3390/ijms17060917

Wang, M., Ma, Y., Sun, Y., Hong, S.Y., Lee, S.K., Yoon, B., Chen, L., Ci, L., Nam, J.-D., Chen, X., Suhr, J., 2017. Hierarchical Porous Chitosan Sponges as Robust and Recyclable Adsorbents for Anionic Dye Adsorption. Sci. Rep. 7, 18054. https://doi.org/10.1038/s41598-017-18302-0

Wehrli, W., 1983. Rifampin: Mechanisms of Action and Resistance. Clin. Infect. Dis. 5, S407–S411. https://doi.org/10.1093/clinids/5.Supplement_3.S407

Winkler, H., Haiden, P., 2016. Treatment of Chronic Bone Infection. Oper. Tech. Orthop. 26, 2–11. https://doi.org/10.1053/j.oto.2016.01.002

Xing Liang, Boppart, S.A., 2010. Biomechanical Properties of *In Vivo* Human Skin From Dynamic Optical Coherence Elastography. IEEE Trans. Biomed. Eng. 57, 953–959. https://doi.org/10.1109/TBME.2009.2033464

Zhang, J., Ma, P.X., 2013. Cyclodextrin-based supramolecular systems for drug delivery: Recent progress and future perspective. Adv. Drug Deliv. Rev. 65, 1215–1233. https://doi.org/10.1016/j.addr.2013.05.001

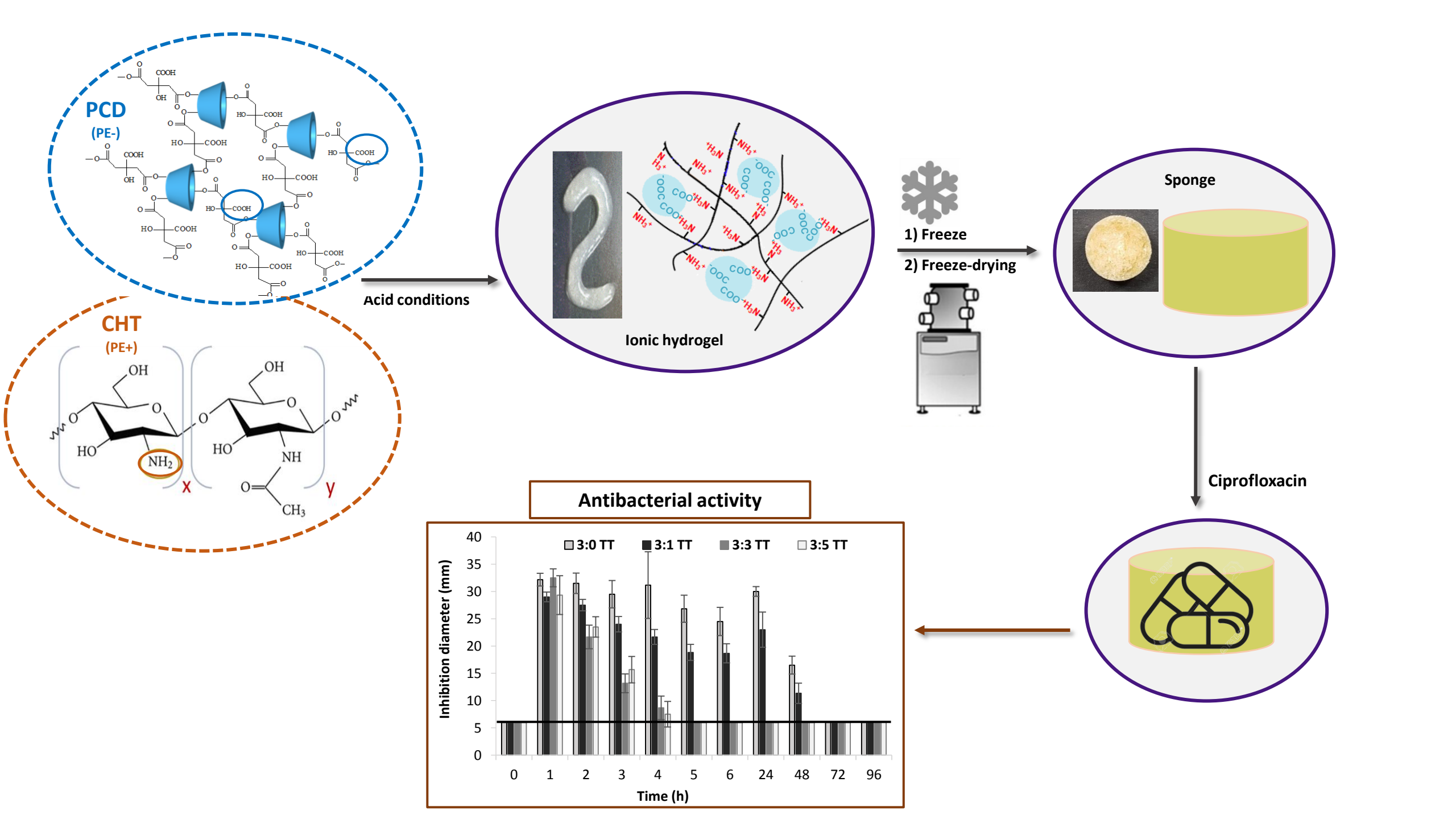
PCD
(PE-)
CHT
(PE+)
Acid conditions
Ionic hydrogel
1) Freeze
2) Freeze-drying
Sponge
Ciprofloxacin
Antibacterial activity
3:0 TT
3:1 TT
3:3 TT
3:5 TT
Inhibition diameter (mm)
Time (h)
0
1
2
3
4
5
6
24
48
72
96